



Alzheimer Disease and Glioblastoma

Expression in Glioma

BY

Maada-Korsu Joseph M Kandeh

G20593108

University of Central Lancashire

A thesis submitted in partial fulfilment for the requirements for the degree of
MSc (by Research) at the University of Central Lancashire

February 2024

RESEARCH STUDENT DECLARATION FORM

Type of Award **Master by Research**

School **Pharmacy and Biomedical science**

*Sections marked * delete as appropriate*

1. Concurrent registration for two or more academic awards

*I declare that while registered as a candidate for the research degree, I have not been a registered candidate or enrolled student for another award of the University or other academic or professional institution

2. Material submitted for another award

*I declare that no material contained in the thesis has been used in any other submission for an academic award and is solely my own work

3. Collaboration

Where a candidate's research programme is part of a collaborative project, the thesis must indicate in addition clearly the candidate's individual contribution and the extent of the collaboration. Please state below:

4. Use of a Proof-reader

*No proof-reading service was used in the compilation of this thesis.

Signature of Candidate



Print name: **Maada-Korsu Joseph M Kande**

ACKNOWLEDGEMENTS

First and foremost, I would like to say thanks to my family, Dr Joseph Kandeh, Kathleen Kandeh and Jenneh Kandeh for supporting me. To my favourite people, my nephew and niece Thomas and Anne-Marie, thank you for giving me the motivation. To my best friend and cousin Fatmata Dalia Katter, thank you for always being there.

To Dr Christopher Smith, thank you for everything you did for me throughout this process. I am extremely grateful for all of it.

Elizabeth Mamie-Baindu Katta, may your soul rest in perfect peace.

Abstract

Alzheimer's disease (AD) is characterised by progressive impairments in memory and cognitive process and contributes to 50 – 70% of dementia cases. Alzheimer's predominantly presents in people over 65 while brain cancer incidence is similarly seen in the elderly. Glioblastoma (GBM) is the most aggressive form of primary malignant brain tumour with life expectancy only 15 months following diagnosis. A relationship between the two neurological diseases was first suggested when patients with AD were found to be less likely to die from cancer compared to AD patients who died from other diseases. Meta-analysis has confirmed that cancer patients have a 50% reduced risk of developing AD with a general consensus of inverse comorbidity. Beta amyloid exists in two main forms A β 40 and A β 42 and has long been at the centre of AD pathogenesis. Our preliminary data suggests it to also be present in glioma. However, the full role of beta amyloid or its associated proteins have not been fully explored in GBM.

Immortalised cell lines U87-mg (human grade IV GBM), SVGp12 (human foetal glial cell) and 1321N1 (human low-grade astrocytoma) were used throughout.

ELISA assay was able to confirm presence of both A β 40 and A β 42 in U87-mg, 1321N1 and SVGp12 cell lysates with no significant difference between the different cell lines. Pharmacological inhibition of beta amyloid similarly had no significant effect on cell proliferation in the glioma cell lines.

Bioinformatic exploration of beta amyloid associated genes was undertaken to identify novel targets to study in the glioma cell lines. BRCA2 and BCHE genes showed different expression in LGG and GBM compared to normal tissue. BRCA2 expression was confirmed in cell lysates by western blot with less BRCA2 in U-87mg and SVGp12 compared to 1321N1.

BRCA2 has been long implicated in other cancers, however the role BRCA2 may have in glioma brain tumours remain unknown. BRCA2 may therefore be an interesting protein for further study and a potential strategy in GBM.

TABLE OF CONTENTS

CHAPTER 1: INTRODUCTION

1	Introduction.....	10
1.1	Alzheimer's.....	11
1.1.1	Diagnosis and Treatment.....	11
1.1.2	Epidemiology.....	12
1.1.3	AD Pathogenesis.....	13
1.2	Glioblastoma.....	15
1.2.1	Diagnosis and Treatment.....	16
1.2.2	Epidemiology.....	16
1.3	Relationship between Alzheimer's Disease and Glioblastoma.....	17
1.4	Quantification of ab40 and ab42.....	18
1.5.	Justification of Methodology.....	19
1.6.	Aim and Objectives.....	21

CHAPTER 2: METHODS

2.1	Cell culture.....	23
2.2	CCK-8 assay.....	23
2.3	Treatment.....	23
2.4	Preparation of cell Lysate.....	24
2.5	BCA Protein assay.....	24
2.6	Enzyme-linked immunosorbent assay.....	24
2.7	Bioinformatics.....	24
2.7.1	Gene identification and analysis.....	24
2.8	Statistics.....	26

2.9	Western blot.....	26
2.9.1	Method development – Amyloid beta quantification.....	26
CHAPTER 3: RESULTS		
3.1	Quantification of A β 40 and A β 42 by western blot and ELISA.....	28
3.1.1	ELISA.....	32
3.2	Effect of amyloid inhibition on glioma cell growth.....	33
3.3	Bioinformatic exploration of amyloid associated proteins.....	36
3.3.1	Expression of <i>BRCA2</i> in glioma.....	37
3.3.2	Expression of <i>BCHE</i> in glioma.....	3
CHAPTER 4: DISCUSSION		
4.1	Amyloid beta as putative target in glioblastoma.....	42
4.2	Technical consideration of A β 40 and A β 42 quantification	43
4.3	Bioinformatics.....	44
4.3.1	BRCA2 and BCHE as new targets in glioblastoma.....	44
4.3.2	<i>BCHE</i>	44
4.4.	CONCLUSION.....	45
CHAPTER 5: REFERENCES		
CHAPTER 6: APPENDIX		

LIST OF FIGURES

1	AD Genes associated to familial AD and Sporadic AD.....	12
1.1	Amyloidogenic and Non-amyloidogenic pathway.....	15
2.1	UCSC Xena – TCGA TARGET GTEX dataset.....	25
3.1	ELISA ab40 and ab42.....	33

3.2	K01-162 drug optimisation.....	33
3.2.1	K01-162 Drug treatment.....	35
3.3	LGG and GBM gene distribution.....	36
3.3.1	<i>BRCA2</i> Gene expression.....	37
3.3.2	<i>BRCA2</i> Kaplan Meier survival analysis.....	38
3.3.3	<i>BRCA2</i> Western blot.....	38
3.3.4	Densitometric analysis of <i>BRCA2</i>	39
3.3.5	<i>BCHE</i> Gene expression.....	39
3.3.6	<i>BCHE</i> Kaplan Meier survival analysis.....	40

LIST OF TABLES

1	Gel and running conditions for Western blot.....	31
2	LGG and GBM gene expression against normal.....	64

LIST OF APPENDICES

1.1	Dot blot stained with ab40 antibody on 1321N1 and U87-mg.....	56
1.2	Dot blot stained with ab42 antibody on 1321N1 and U87-mg.....	56
1.3	Ponceau S stain on nitrocellulose membrane.....	57
2.1	ELISA ab40.....	58
2.2	ELISA ab42.....	59

2.3.	Drug optimisation.....	60
2.4	Drug treatment.....	61
3	LGG and GBM gene expression against normal.....	62
3.1	LGG gene expression against normal samples distribution.....	64
3.2	GBM gene expression against normal samples distribution.....	65
3.3	List of 30 genes used for distribution.....	66
4.	Buffers.....	67

Abbreviation

α KG	α -Ketoglutarate
A β	Beta amyloid
ABO	Beta-amyloid oligomers
ACh	Acetylcholine
AChEIs	Acetylcholinesterase inhibitors
AD	Alzheimer disease
APP	Amyloid precursor protein
BA	Beta-Amyloid
BRCA2	Breast Cancer Gene 2
BCHE	Butyrylcholinesterase
ChAT	Choline Acetyltransferase
CNS	Central nervous system
CO ₂	Carbon Dioxide
D-2HG	D-2-Hydroxygluterate dehydrogenase
DDR	DNA Damage Response
DNA	Deoxyribonucleic acid
ELISA	Enzyme Linked Immunosorbent Assay
ERK	Extracellular Signal-regulated Kinases
FAD	Familial Alzheimer disease
FBS	Foetal Bovine Serum
GBM	Glioblastoma
GSK	Glycogen Synthase Kinase
HR	Homologous Recombination
IDH	Isocitrate Dehydrogenase
LGG	Low grade glioma
MAPT	Microtubule-Associated Protein Tau
NADP	Nicotinamide Adenine Dinucleotide Phosphate
NADPH	Nicotinamide Adenine Dinucleotide Phosphate
NFT	Neurofibrillary tangle
NMDA	N-methyl-D-aspartate
NS	No Statistical Difference
PKR	Protein Kinase C
PSEN 1	Presenilin-1
PSEN 2	Presenilin-2
RAD51	RAD51 Recombinase
RIPA	Radioimmunoprecipitation assay buffer
SAD	Sporadic Alzheimer disease
TCA	Tricarboxylic Acid Cycle
TMZ	Temozolomide
WHO	World Health Organisation

Chapter 1

Introduction

1.1 Alzheimer's Disease

The words “*A peculiar severe disease process of the cerebral cortex*” was said by Alois Alzheimer on November 3rd, 1906, on the 37th meeting of the southwest German Psychiatrists in Tübingen. The words describing a 50-year-old woman who showed symptoms reported by Alois Alzheimer's as “paranoia, progressive sleep and memory disturbance, aggression, crying and progression confusion” (Hippius, 2003). Five-years after the death of the woman, the histology of the brain reported plaques and neurofibrillary tangles (Hippius, 2003). One hundred years later Alzheimer diseases (AD) falls under the umbrella of a dementia characterised by progressive impairments in memory and cognitive process (McGirr et al., 2020) and is described as the aggregation of beta amyloids ($A\beta$) and hyperphosphorylated tau accumulation in extracellular plaques leading to neurotoxicity (Liu et al., 2020).

1.1.1 Diagnosis and treatment

The current clinical diagnosis of AD is a cognitive test appropriate for the patients age and education, followed by the elimination of differential diagnosis (mainly eliminating dementia) and followed by position emission tomography (PET) for the presence of cerebral cortical atrophy (Schott and Petersen, 2015) (Bird, 2012).

As of yet there is no cure for the disease, the only treatment to combat the disease is to relieve symptoms or reverse the effect of neuronal deaths that leads to imbalance or lack of neurotransmitters such as acetylcholine, dopamine and serotonin (Yiannopoulou and Papageorgiou, 2020). The main treatment is acetylcholinesterase inhibitors (AChEIs) to slow down the cognitive decline in AD. The cholinergic hypothesis states the loss of cholinergic function in the central nervous system (CNS) as seen in AD affects cognitive decline such as memory and learning (Terry and Buccafusco, 2003). The three cholinesterase inhibitors approved for the treatment of AD are donepezil, galantamine and rivastigmine. The acetylcholinesterase inhibitors work by increasing the neurotransmitter at synapses by decreasing its breakdown rate (Colovic et al., 2013) which has been proven to delay cognitive decline in AD in some instances (Yiannopoulou and Papageorgiou, 2020). The only other clinical drug approved for the treatment of AD that acts on a different pathway to AChEIs is memantine. The drug is a N-methyl-D-aspartate (NMDA) receptor antagonist used to reduce excitotoxicity by decreasing the influx of Ca^{2+} . The drug only binds to open NMDA receptors during prolonged activation allowing the normal activity of the receptor (Yiannopoulou and Papageorgiou, 2020). As well as clinically approved drugs, drug trials are a major weapon used to fight the disease, 121 unique therapies as of February 2020 in clinical trials from phase 1 to phase 3 for AD (Cummings et al., 2020). In 2023, the Food and Drug Administration (FDA) approved Lecanemab an IgG1 monoclonal antibody for the treatment of AD (Verger et al., 2023). In addition, the pharmaceutical company Eli Lilly have applied for approval by the FDA for the drug Donanemab which is also a monoclonal antibody (Reardon 2023). Donanemab is said to have 35% less clinical decline over 18 months in comparison to Lecanemab which showed a 27% decline over 18 months. The FDA prescribing guidelines includes warnings of amyloid related imaging abnormalities (ARIA) as MRI showed up to 21% of patients in Lecanemab

trial presented with ARIA which includes brain swelling or brain bleeding. In Donanemab 37% presented with ARIA (Sanganeer 2023, Couzin-Frankel, 2023).

1.1.2 Epidemiology

There are around 55 million people with dementia worldwide (WHO, 2021), with AD contributing to 50-70% of the cases (Zhang et al., 2021). The total cases are said to increase to 78 million by 2030 as life expectancy increases and 139 million in 2050. Most people with dementia (60%) reside in less to medium developed countries. In addition, women make up 65% of death due to dementia. As nearly a billion people are said to be over 65 by 2030 compared to 420 million in 2000 (Zhang et al., 2021) (Qiu et al., 2022), this ageing phenomenon will increase the crisis that is dementia in general and subsequently AD as age is one of the risk factors to dementia. As the high developed countries show a greater aging population increase (59% - 71%), those countries will show the greater increase of people with dementia (Qiu et al., 2022). The elevated prevalence of AD in women compared to men implies that age alone cannot be the sole factor. Despite women having a longer life expectancy than men, with a median age of 86 compared to 82 (Office of National Statistics, 2021), research indicated oestrogen may serve as a protective factor against AD (Saleh, 2023). Consequently, the decline in oestrogen levels due to menopause could contribute to the higher prevalence rate observed in women. It's important to consider that hormonal therapy has been associated with an increased risk of dementia (Shumaker, 2004)

AD can be split in to two groups, Familial Alzheimer's disease (FAD) and Sporadic Alzheimer's disease (SAD). FAD predominantly occurs in individuals <65 years accounting for 5% of AD and SAD affects individuals >65 years (Binda, 2019).

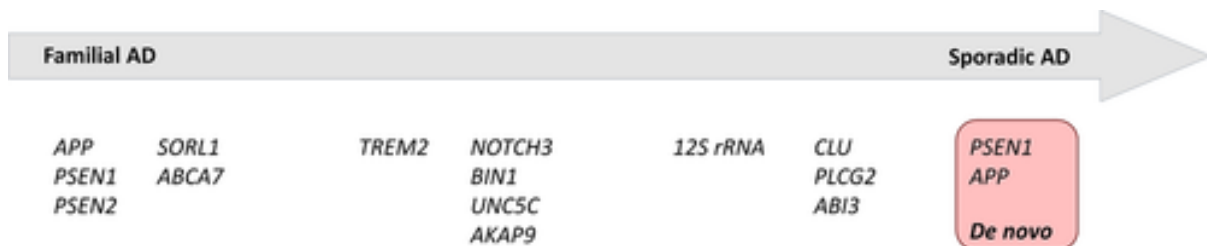


Figure 1; Spectrum showing FAD and SAD of genes associated to the two groups deduced via minor allele frequency (MAF) <1% (Hoogmartens et al., 2021)

Figure 1 shows the genes most well characterised associated to the groups, as seen APP and PSEN1 are highly linked to both FAD and SAD. There are several hypotheses for the disease, but none blankets every point. It is worth noting the genes in Figure 1 only represent minor alleles, APOE ϵ 4 is a major genetic risk factor in AD. Although the mechanism is not clear the allele significantly contributes to the reduction of A β clearance (Kim et al., 2009 & Liu et al., 2013).

1.1.3 AD pathogenesis: Cholinergic hypothesis

This hypothesis was first introduced in the mid-1970s when research in biochemical side of Alzheimer's disease began in late 60s to early 70s. Reports started coming through of the decrease in expression of choline acetyltransferase (*ChAT*) in the neocortex. The deficit was seen to lead to a reduction of choline uptake, acetylcholine (ACh) release and loss of cholinergic nerve perikaryon (Francis et al., 1999). The role of ACh in learning and memory compounded with the studies of these deficits lead to the cholinergic hypothesis. Although the hypothesis does correlate with the memory loss seen in AD it does not necessarily paint the full picture. The decrease in expression of *ChAT* in AD is also seen in olivopontocerebellar atrophy (OPCA) patient but without the cognitive decline (Francis et al., 1999, Kish et al., 1993) suggesting that other factors must contribute to the memory loss seen in AD patients.

sAPP α is a fragment derived from APP through proteolytic cleavage. APP is a transmembrane protein primarily found in the membrane of neurons. sAPP α is generated when APP is cleaved by alpha-secretase, an enzyme that cuts within the A β domain of APP. This cleavage event precludes the formation of A β peptides, which are implicated in the pathogenesis of AD.

The cholinergic system has been seen to play a vital role in the pathogenesis of AD. Stimulation of the M1 receptor by an agonist increases the soluble amyloid precursor protein alpha (sAPP α) and reduce A β production (Jiang et al., 2014, Haring et al., 1994). M1 also activates Protein Kinase C (PKC) which could lead to the inactivation of protein kinase (GSK-3) therefore reduces hyperphosphorylated tau (Sadot et al., 1996, Francis et al., 1999, Jiang et al., 2014). *In vivo* and *in vitro* studies have showed a decrease of neuronal degeneration and death when *GSK3 β* was inhibited (Forlenza et al., 2000, Mendes et al., 2009, Noble et al., 2005). Furthermore, stimulation of mAChR could activate ERK1/2 pathway, which plays a role in α & γ - secretase and app processing (Jiang et al., 2014, Zhang et al., 2019).

1.1.4. AD Pathogenesis: Tau hypothesis

The discovery of phosphorylated tau proteins being the building blocks of neurofibrillary Tangles (NFT) by KOSIK et al (1986) ignited the Tau hypothesis. The claim is that Tau accumulation precedes that of A β , making it the instigator that leads to a cascade resulting in cell death. The hypothesis is supported by hyperphosphorylated Tau being found in brains of individuals with mild dementia without A β (Yilmazer-Hanke et al., 1999, Mandelkow et al., 2007, Mazanetz et al., 2007). Unlike the amyloid cascade hypothesis, the Tau hypothesis has no genetic mutation in the Microtubule-associated protein tau (*MAPT*) gene that can be associated to the disease. *MAPT* gene is responsible for the encoding of tau proteins. The protein is responsible for maintaining the structural integrity of microtubules, due to disruption of tau kinases and tau phosphatases equilibrium tau proteins become hyperphosphorylated causing the disruption of microtubules which

leads to free tau aggregating (Medeiros., 2011). The aggregation of tau proteins binds with free A β forming NFT.

1.1.5. Amyloid cascade hypothesis

Breakthrough of the disease pathogenesis was discovered by Glenner and Wong (1984) when they isolated a protein now known as A β 42, they believed A β 42 is a “*biological marker for the cerebrovascular amyloid fibril component of Alzheimer’s disease*”. As cerebrovascular amyloidosis was only seen in AD, Down syndrome and familial Icelandic cerebrovascular amyloidosis syndrome, Glenner and Wong assumed that isolating and identifying the protein that is the cause would lead to diagnostic factor of AD. This research laid the building blocks for future therapeutic pathways based on the Amyloid cascade hypothesis.

Although there are still questions about the pathogenesis of AD as a whole as no hypothesis or model represents the entirety of the disease, the consensus on the cause of FAD is the Amyloid cascade hypothesis, which was first proposed by Hardy and Higgins in 1992. The authors hypothesised that the accrual of A β is the cause of AD. This hypothesis is backed by the mutations of APP, Presenilin-1 (PSEN1) and Presenilin-2 (PSEN2) genes that lead to an increase production of A β 42 which leads to neurofibrillary tangles and cell death in FAD.

The amyloidogenic pathway is the biogenesis of A β which involves the cleavage of APP by β -secretase (BACE) and γ -secretase to produce A β . Newly synthesized APP molecules are transported from the Golgi either down the axon to synaptic terminals or via an endosomal compartment. APP transported to the cell surface can be proteolyzed at the surface. APP not proteolyzed at the surface can then be reinternalized via clathrin-coated pits in endosomal compartments containing β -secretase enzyme 1 (BACE1) and γ -secretase (a multimeric complex consisting of presenilin, nicastrin anterior pharynx defective-1 and presenilin enhancer-2). In the endosome BACE1 initiates the first proteolysis step cleaving APP releasing a N-terminal ectodomain sAPP β fragment and a membrane bound 99-amino acid C terminal fragment (C99) (Vassar et al., 1999). γ -secretase then cleaves C99 releasing A β extracellularly and APP intracellular domain (AICD). In non-amyloidogenic pathway α -secretase initiates the first step in this pathway, cleaving APP and producing the soluble APP α and Carboxyterminal fragment 83 (CTF83). γ -secretase then cleaves the fragment producing p3, A β and AICD (Chow et al., 2010). This process is accepted as the non-amyloidogenic pathway as A β is not generated at the end. This process is seen in figure 1.1.

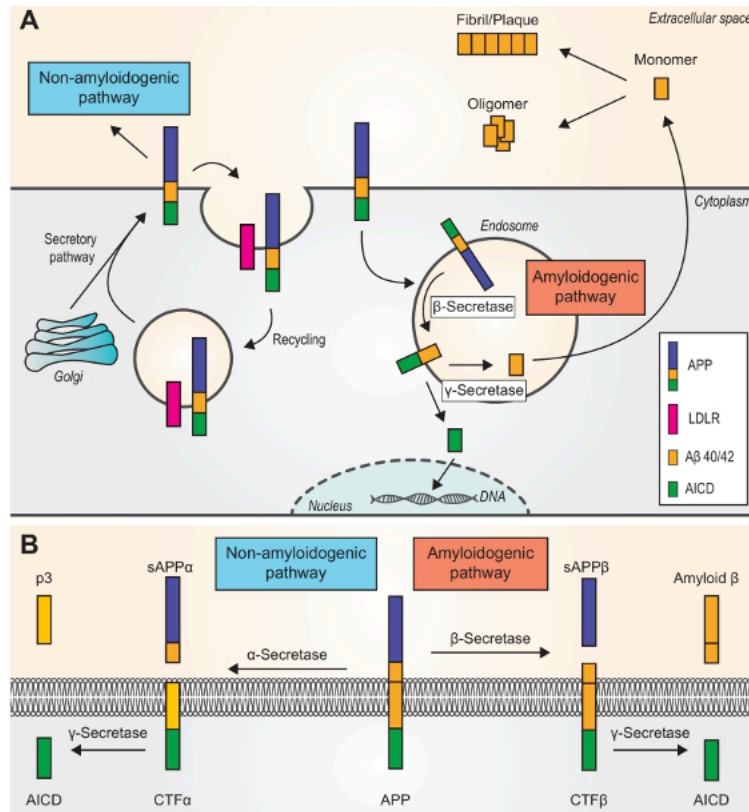


Figure 1.1: this image shows both the amyloidogenic and non-amyloidogenic pathway. Section A of the image shows the intracellular cascade of both pathways as explained above. Section B is the simplified version of the pathways (Zhou et al 2018).

The major drawback of the hypothesis is the fact that several manufactured Aβ antibodies had failed to reduce cognitive decline in phase III trials until recently. Moreover, it has been seen individuals with Down syndrome develop Aβ plaques as adolescents and never progressed to AD (Zigman et al., 2008). There's no question that Aβ facilitates AD but it is not exclusively the cause of the disease.

1.2 Glioblastoma

Cancer is an uncontrolled division of cells that can invade and spread throughout the body. Hallmark of cancer is a phrase used as a benchmark for all cancer, the belief is every cancer has the abilities to sustain proliferative signalling, evade growth suppressors, activate invasion and metastasis, enable replicative immortality, induce angiogenesis and resist cell death (Hanahan and Weinberg, 2011).

Glioma is a tumour originating from glial cells in the central nervous system (CNS). The tumour is accountable for 50% of all primary malignant brain tumours (Lan, et al., 2017). Astrocytoma derives from astrocytes, ependymoma arising from ependymal cells and oligodendroglioma emerging from oligodendrocytes make up the three main types of glioma. Glioblastoma is a particularly aggressive astrocytoma and is the most prevalent primary malignant tumour in adults.

1.2.1 Glioblastoma classification

Prior to 2021 GBM was divided into two types of groups; primary glioblastoma which is a grade IV de novo whilst secondary glioblastoma is a progressive development from a lower grade astrocytoma to a grade IV. WHO has since changed the classification of the disease into *IDH* wild-type and *IDH* mutant. The old classification was based on the histology findings and / or glomeruloid neovascular proliferation and pseudopalisadic necrosis (Stoyanov et al., 2022, Wen et al., 2021). The new classification is based on lack of *IDH* mutation. The changes of the classification was due following the realisation patients with the mutation have a much better prognosis (42 months) compared to patients with *IDH* wild-type (14 months) (Alzzial et al., 2022).

Isocitrate dehydrogenase (*IDH*) are enzymes found in the cytoplasm, peroxisomes and mitochondria and comprise three isoforms *IDH1*, *IDH2* and *IDH3*. These are metabolic enzymes involved in several different cellular processes. In reference to glioma the enzymes are involved in the tricarboxylic acid cycle (TCA cycle) which is the major energy-yielding metabolic pathways in glioma. *IDH1* and 2 are responsible for catalysing isocitrate to α -ketoglutarate (α KG) and reducing nicotinamide Adenine Dinucleotide Phosphate + (NADP+) to Nicotinamide Adenine Dinucleotide Phosphate (NADPH) + CO₂ (Mondesir et al., 2016). The reducing agent NADPH is important in processes that protect against toxic reactive oxygen species and oxidative damages via the reduction of glutathione, thioredoxins and activating catalase.

IDH mutants occur due to a missense mutation, substituting arginine 132 in *IDH 1* and arginine 172 or 140 in *IDH 2* which subsequently play an important role in the enzymes active site. The change in the enzyme reduces its function in converting isocitrate to α KG. Furthermore, the missense mutation causes *IDH* mutants to inhibit *IDH* wild-type (Zhao et al., 2009). *IDH*-mutant enzymes exhibit neomorphic enzymatic activity by transforming NADPH and α KG into NADP+ and D-2-Hydroxygluterate dehydrogenase (D-2HG). D-2HG inhibits α KG in a mild competitive manner and therefore increasing histone methylation, increasing DNA methylation and impairs cell differentiation (Mondesir et al., 2016). Furthermore, inhibiting the production of NADPH increases radiation therapy sensitivity (Tateishi, et al., 2016). In 2016 WHO revised the classification of glioblastoma due to *IDH* into *IDH* mutant and *IDH* wild type for glioblastoma (Stoyanov et al., 2022).

1.2.1 Diagnosis and Treatment

The clinical presentation of glioblastoma is ambiguous which unfortunately decreases the likelihood of a timely diagnosis and favourable prognosis. The disease exhibits symptoms parallel to that of other primary and secondary brain tumours including headache, blurred vision, seizure, and cognitive decline. Due to early signs aligning with majority of condition an early diagnosis of the disease is highly unlikely which is detrimental to course of treatment and prognosis.

Diagnosis of the disease depends on clinical presentation and a thorough evaluation of family history, ruling out other conditions such as intracranial pressure. Even though the initial route of diagnosis for patients is different depending on their symptoms, every patient would eventually have a Magnetic Resonance Imaging (MRI) scan which will present blood-brain barrier disruption, necrosis and vasogenic oedema or infiltrating tumour (McKinnon et al., 2021). A confirmation of the disease is then done via biopsy for a histopathological diagnosis depending on whether it's considered high risk to a patient.

Treatment of glioblastoma involves removal of tumour depending on the location and size, followed by radiotherapy and temozolomide (TMZ) and then adjuvant TMZ (Stupp et al., 2007). Surgery is dependent on the Karnofsky scale (>70) (McKinnon et al., 2021 & Gilard et al., 2021). In addition, as the median survival rate after diagnosis is 15 months, patients commonly sign up for therapeutic trials, however survival remains poor (Gilard et al., 2021).

1.2.2 Epidemiology

The global incidence rate of glioblastoma has increased yearly and is now between 1-5 per 100,000 people (Grench et al., 2020). The increase of the incidence rate yearly can be explained by medical advances, or in contribution of environmental factors such as pollution. Studies show western world, such as the UK with an incidence rate of 5 per 100,000 is greater than less developed countries. This could be because of poor access to health care therefore a decrease in reported cases. Interestingly only Japan has showed a decrease in incidence rate (Miranda-filho et al., 2016). In the UK a greater prevalence of glioblastoma is seen in men compared to women and a year-on-year increase across different ages (Philips et al., 2018).

1.3 Relationship between Alzheimer's disease and Glioblastoma

AD and GBM are two neurological diseases that have significantly impacted humans, particularly the elderly populations, showing a contrasting comorbidity pattern.

The link between AD and cancer was first found following an analysis of autopsy results where 9% patients with AD had cancer contributing to death. Moreover, 23% had cancer contributing to their death out of patients without AD (Tirumalasetti et al., 1991). It is worth noting that the sample size of was small even though a trend in favour of inverse comorbidity was seen.

A study showed a significantly lower rate in female patients with AD in co-occurrence of cancer (Thorpe et al., 1994). In the same year another study concluded no significant difference in AD with cancer such as lung or prostate cancer, furthermore, the occurrence of pancreatic cancer was 6.7-fold higher in Alzheimer's than in control subjects (Burke et al., 1994).

Since then, there have been growing consensus of an inverse relationship between AD and cancer. In northern Italy a study was done by Musicco et al (2013) that showed the cooccurrence of cancer in AD patients had a 50% reduction risk and a 35% reduced risk of AD in cancer patients. A longitudinal study of 5888 individuals in a 10-year period mirrored the same conclusion of a reduced risk of developing AD in patients with cancer (Roe et al., 2010).

A meta-analysis showed a 50% reduced risk of AD in patients with or history of cancer and a 36% reduced risk of cancer in patients with AD (Catala-lopez et al., 2014) which might be because both diseases share or express the same genes or pathways in opposite direction (Ibanez et al., 2014) therefore explain the protective barrier shown by the diseases.

A mechanistic relationship between AD and glioblastoma was suggested when reduced production of A β was seen in C6 glioma cell line (Morato and Mayor, 1993) while *in vivo* suppression of tumour growth was demonstrated by human glioblastoma A β in mice (Paris et al 2004).

As widely accepted the pathogenesis of AD is the aggregation of A β and hyperphosphorylated tau proteins accumulating in extracellular plaques leading to neurotoxicity (Holtzman et al., 2011). Interestingly, Tau protein has also been seen to facilitate tumour progression in nude mice (Pagano et al., 2021). Pharmacological interference of Tau signalling pathway has been suggested as a novel treatment for AD as it leads to inhibition of neurofibrillary tangles (Long et al., 2021 & Kitagishi et al., 2014) and may a putative target in cancer.

1.4 Quantification of A β 40 and A β 42

The separation of beta amyloids using conventional SDS page has been difficult to do, using Bicine/Tris SDS page (15%T/5%C) or Tricine/ Tris SDS page the beta peptides appear in a single band showing no separation (Klafki et al., 1996). The addition of urea to the SDS separation gel showed a clear separation of peptides, it was deduced that A β 40 moved faster in Tris/Bicine/urea SDS page (Klafki et al., 1996). Since then the separation of the peptides allowing quantification has been achieved using different concentration of stacking or separating gel with urea.

In nerve endings of monkeys, A β 40 showed an increase of 3.7 times with age from 4y to 30y whilst A β 42 showed a greater increase of 5 times more (Kimura et al., 2005). A β (A β 40 and A β 42) have been successfully separated and semi quantified in several cells or tissues such as human embryonic kidney cell lines and homogenised cortex and hippocampus using western blotting (cui et al., 2017; Winkler et al., 2012). As of yet there is no data on quantification of A β 40 and A β 42 in glioma cell lines even though the proteins have been identified in glioma cell lines.

1.5 Justification of Methodology

To explore the role of between beta amyloids and glioma cell lines, a literature review was conducted to examine the methodologies used for quantifying beta amyloids in cell lines through western blot analysis.

The quantification of A β 40 and A β 42 by western blot has been done by others on several cells and tissues such as HEK293, frozen cortex and hippocampus and homogenised occipital lobes (Kimura et al., 2005, Klafki et al., 1997, Cui et al., 2011). Although the literature used different methodology to quantify beta amyloid, however despite A β significant presence in neuroscience research, western blot quantification is not routine. Various methods have been reported and six will be outlined here.

1.6.1 Klafki et al. (1996): Electrophoretic separation of B-amyloid peptides A β 40 and A β 42

In 1996, Klafki and colleagues used electrophoresis to successfully separate proteins HEK 293 cells using 3 different types of gels. The gels were run at 12mA for 30 mins, followed by 24mA until the dye reached the appropriate distant. Electrophoresis was done at room temperature. The sample buffer used for electrophoresis was a tris/tricine buffer. The gels were then fixated and stained.

The first gel used to separate the proteins (A β 40 and A β 42) was a gradient gel composed of stacking gel (4%), separating gel (10%) and a resolver gel (16.5%). The gel was made from acrylamide/bis, tris/ HCL gel buffer, glycerol, Coomassie blue, APS, TEMED and water. The anodic buffer used was Tris/ HCL and cathodic buffer was Tris/tricine/SDS. Using this gel, the band of A β 40 and A β 42 was successfully stained with A β 40 producing an intensified band to its counterpart. As a mixture of the two, the bands were unable to be separated using this gel composition.

The second gel used for electrophoresis was gradient gel made up of stacking gel, separating gel and resolver gel (15%). The anodic buffer used was Tris/ H₂SO₄ and cathodic buffer was bicine/NaOH/SDS. The buffer used for stacking gel consisted of bistris / bicine and bromophenol blue, for separating gel was bistris / H₂SO₄ and for resolver gel was Tris / H₂SO₄ and glycerol. The gels also consisted of acr/bis, SDS, H₂O, APS and TEMED.

The result seen was similar to the first gel, A β 40 band appeared more intense than A β 42 and as a mixture the bands could not be separated.

The third gel used for electrophoresis was also a gradient gel made up of stacking gel, separating gel and resolver gel (15%). The anodic buffer used was Tris/ H₂SO₄ and cathodic buffer was bicine/NaOH/ and a higher concentration of SDS. The buffer used for stacking gel consisted of bistris / bicine and bromophenol blue, for separating gel was bistris / H₂SO₄ and for resolver gel was Tris / H₂SO₄ and urea. Unlike the first two gels, different mobilities of A β 40 and A β 42 was seen in the mixture of the stains, pointing to urea as a facilitator of the separation of the two

proteins. Urea is a chemical that breakdowns hydrogen bonds therefore increasing solubility of proteins (Bass et al., 2017). Similar results were seen a year later, when Wiltfang et al., 2017 found that urea and SDS increase the mobilities of proteins. Using bicine/tricine gel with and without urea, A β 40 and A β 42 separated more convincingly with the former.

1.6.2 Zhong et al. (1994): Increased Amyloid production from Aberrant B-Amyloid Precursor Proteins

A 16.5% Tris-Tricine SDS-PAGE was used in electrophoresis to detect β -APP carboxyl-terminal fragments, the gels were then developed using autoradiography. Unfortunately, the running buffer used were not specified, nonetheless the results showed fragments at around 4kda which A β 40 and A β 42 are and fragment at around 3 kda (Zhong et al., 1994).

1.6.3 Ahmed et al (2010): Structural conversion of neurotoxic amyloid-B1–42oligomers to fibrils

The Ahmed, 2010 methodology looked at separating A β 42 oligomers. Samples of A β 42 oligomers (incubated for 6h at 4 °C) were mixed with SDS-PAGE sample buffer and loaded onto 18% (w/v) Tris-glycine poly-acrylamide gels, electrophoresed and transferred onto Hybond-ECL nitrocellulose membranes at 100V for 1.5h at 4°C. Membranes were blocked in 5% (v/v) milk/PBS/0.05% (v/v) Tween20 (PBS-T) for 1h at room temperature (22°C). Anti- A β mouse monoclonal antibody 6E10 was added for 1h at room temperature and then washed away in three 5-min washes with PBS-T. Horseradish peroxidase–conjugated mouse sheep anti–mouse IgG was added for 1h at room temperature and then washed three times for 5 min with PBS-T. ECL detection method was used for detection of the bands. Molecular sizes for immunoblot analysis were determined using a Benchmark pre-stained protein ladder and Rainbow molecular weight markers. For native gels, samples were loaded onto 10–20% (w/v) Tris-tricine native gels (Bio-Rad) electrophoresed at 4 °C and visualized with Coomassie brilliant blue stain (Sigma-Aldrich). Molecular weights for native gel analysis were approximated using NativeMark molecular weight standards (Invitrogen) (Ahmed et al., 2010).

1.6.4 Kimura et al. (2005): Age-related changes of intracellular A β cynomolgus monkey brains

Western blot analyses were performed to assess age-related changes in the subcellular distribution of each A β molecule. The nerve ending fraction was pre-treated with Pro-K as described. The proteins in each fraction were adjusted to 30 mg, and then each fraction was analysed by using SDS polyacrylamide gel electrophoresis (SDS PAGE using 12.5% acrylamide gels). Separated proteins were blotted onto polyvinylidene fluoride membranes. The membranes were blocked with 5% non-fat dried milk in 20 mM PBS (pH 7.0) and 0.1% Tween-20 overnight at 4°C, and then incubated with primary antibodies or 1h at room temperature. They were then incubated with either horseradish peroxidase-conjugated goat anti mouse IgG or mouse anti rabbit IgG for 1h at room temperature (Kimura et al., 2005).

1.6.5 Cui et al. (2017): Peripheral Treatment With Enoxaparin Exacerbates Amyloid Plaque Pathology in Tg2576 Mice

Frozen cortex and hippocampus were homogenized with a disposable polypropylene pestle (Bio-Rad) in 1ml sample buffer (10% b-mercaptoethanol, 2% SDS, 50mM Tris, and 10% glycerol, pH 6.8). Samples were sonicated for 4 min and centrifuged for 10 min at 13,000 rpm at 4°C, and then the supernatant fraction was collected. The protein concentration was measured with the Bio-Rad DC protein assay kit with bovine serum albumin as standard. The authors based their method on Cui et al., (2011) (1996)

1.6.6 Haider et al. (2012): Tricine-SDS-PAGE

This chapter was written as a guide for separating small proteins, predominantly 1 – 30kda using tricine SDS PAGE. The method included making hand cast gels. The buffer used for making the gel was a 2.5M Tris-HCL (ph 8.8) which composed of tris base, deionized water and HCL. The loading buffer was made up of SDS, glycerol, coomassie brilliant blue, Tris-HCL (ph 6.8) and 4% mercaptoethanol. Running buffer consist of tris, tricine and SDS. A gradient gel was the preferred method with 6M urea in the resolver gel, but an updated version of the method was done without the use of urea (Appendix Image 2) (Haider et al., 2012).

1.6 Aim and objectives

The overarching aim is to explore the role of A β oligomers (A β 40 or A β 42) in GBM cells. To this end, the following objectives will be met.

1. To quantify A β 40 and A β 42 in glioblastoma cell lines via western blot and Enzyme Linked Immunosorbent Assay (ELISA)
2. To determine the sensitivity of GBM cells to anti-amyloid drugs.
3. To apply bioinformatics to identify AD susceptible genes in LGG and GBM using public datasets
4. Confirm the expression of identified AD susceptible genes via western blot in glioblastoma cell lines

CHAPTER 2

Method

2.1. Cell culture

Cell lines used were U87-mg (ECACC) which is a grade 4 malignant glioblastoma cell line, 1321N1 a grade 2 human brain astrocytoma and SVGp12 (human foetal glial cell line). U87-mg and 1321N1 were originally purchased from ECACC, UK, SVGp12 from ATCC, UK and stored in liquid nitrogen until being grown under standard cell culture conditions. U87-mg and SVGp12 were grown in Eagle's Minimum Essential Medium (EMEM), with 2mM glutamine, 1% non-essential amino acid, 1mM sodium pyruvate and 10% (w/v) foetal bovine serum (FBS). 1321N1 was cultured in Dulbecco's Modified Eagle Medium (DMEM), 2mM glutamine and 10% (w/v) FBS. Cell culture was performed in Class II microbiological safety cabinet. Cell lines were grown in T75. Cells were washed with Phosphate buffered saline (PBS) after old medium was discarded. The cells were washed twice in 5ml PBS and then trypsinised in 2ml Trypsin and placed in an incubator for 2-3 minutes. The flask was placed under a inverted light microscope to observe dissociation. In the laminar flow hood, the 4/5ml of medium was then added to flask to neutralise the trypsin. The content of the flask was then transferred to a 50ml falcon tube and centrifuged for 12000 xg for 5 minutes. The supernatant was then discarded, and the pellet resuspended in an appropriate volume of medium for seeding. Aseptic technique was used in the entirety of cell culture. The Media and supplements, Foetal bovine serum (FBS), Glutamine, Non-Essential Amino Acids (NEAA), Sodium Pyruvate were bought from Fisher Scientific, UK.

2.2 CCK-8 Assay

CCK-8 assay is a colorimetric assay that determines cell proliferation. This is done by a direct proportionality of living cells to formazan dye, which is a principal product of WST-8 following reduction by dehydrogenase. The assay was bought from Abcam and used according to manufacturer's instruction for cell proliferation. 96 well plates were seeded with 1×10^3 cells in triplicates for each day in the 96 well plate and triplicate of the 96 well plate. Every day the respective wells medium was discarded and then replaced with 10% CCK-8 reagent in growth medium and incubated for 60 minutes. Then the absorbance was read. The Plate reader could only be set to 485nm absorbance instead of 460nm that was instructed.

2.3 Treatment

Cells were treated with the β -amyloid oligomer inhibitor (K01-162). K01-162 bought from Merck (UK) and was stored in the fridge a 4°C. The drug was solubilised in DMSO (50mg/ml) and then diluted using medium to 100 μ M in 10% DMSO and stored in aliquots of 200ul in fridge a 4°C. The cells were treated at concentrations between 1nM to 1 μ M. 96 well plates were used for cell treatment, the wells contained 5×10^3 cells in 100ul volume of medium (1% DMSO and the relevant drug concentration). In their respected medium containing 1%DMSO and 100nM of K01-162 treated cells were seeded per wells in 96 well plate. The respective wells were treated with 10% CCK-8 reagent in DMEM/ EMEM and incubated for 60 mins every day. The absorbance was measured daily, at the same time for 7 days.

2.4 Preparation of cell lysate

Cells at 80% confluency in a T75 flask were trypsinise, neutralise and centrifuge at 1000rpm for 5 minutes. The supernatants were discarded and resuspended in cold 1ml cold PBS. The cell suspension was transferred to an eppendorf tube and spin down for 5 minutes at 14,000xg. The supernatant was then discarded and cells were lysed in 200ul of Radioimmunoprecipitation assay buffer (RIPA buffer) containing 1x protease inhibitor (50mM Tris, 150mM NaCl 0.5% sodium deoxycholate and 1% Triton to make up 50ml of RIPA buffer). 1x protease inhibitor (100ul) was added to 10ml RIPA prior to lysing.

2.5 BCA Protein assay

Bicinchoninic acid (BCA assay) was used to determine the protein levels in cell lysates for western blot and ELISA. The assay was bought from Thermo Fisher and was used according to manufacturer's instruction.

2.6 Enzyme-linked immunosorbent assay (ELISA)

A β 40 and A β 42 in cell lysates were assayed using human ELISA kit (Thermo Fisher, UK). Three different passages of each cell line were assayed in triplicate. A β 40 (25ul of cell lysates) and A β 42 (50ul of cell lysates) was quantified and was measured at an absorbance of 485nm. The assays were bought from Thermo Fisher and used according to manufacturer's instruction.

2.7 Bioinformatics

2.7.1 Gene identification and analysis

GeneCards (Genecards, 2022) is a genomic database that was used to rank closely linked genes to beta amyloid and glioblastoma. The website does this by quantifying genes linked to anything like another gene or protein or disease in publications, therefore when a gene is searched or diseases, A list of genes is generated in order of the most associated gene to the least. In gene cards, beta amyloid and glioblastoma were searched, and the top 100 genes were selected for beta amyloid and 23 for glioblastoma. To analyse the gene expression of the top selected genes that are closely link to beta amyloid and glioblastoma, USCS Xena browser (Xenabrowser, 2022) was used.

The datasets TCGA, TARGET and GTEX were filtered to brain as the primary site and the main category stratified into low grade glioma (LGG), glioblastoma (GBM)

and GTEX (normal tissue). This gave 530 LGG samples, 172 GBM samples and 1141 normal tissue samples (see Figure 2.1).

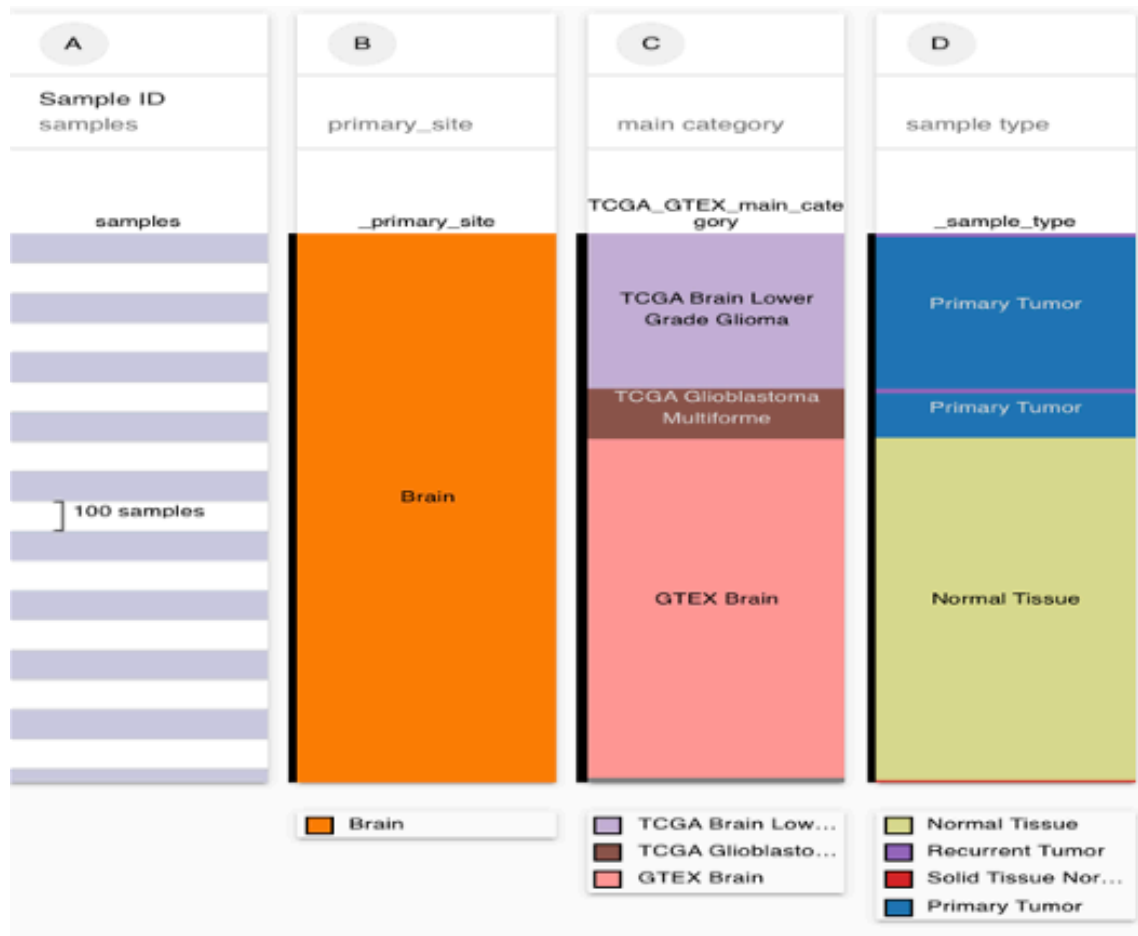


Figure 2.1; TCGA TARGET GTEX data, 3 categorise, primary site, main category and sample type

The aim of the analysis was to filter down the genes. The average of the gene expression of the raw patient sample data was done for each individual gene. Then, GBM and LGG average gene expression of each gene were divided by the control counterpart and multiplied by 100 (Appendix 3, Table 1). i.e. average of APP gene expression of GBM data divided by the average of APP GTEX expression data and then multiplied by 100. This was done to see how close in expression the gene is in control data compared to GBM and LGG. The closer to 100% meant the genes were closely expressed. A bell chart (Appendix 3, Figure 3.1, 3.2) was then created from the data to show the anomalous genes either side of the spectrum. Genes with over 130% (21 genes) and those with below 70% (32 genes) were identified for both LGG and GBM. The threshold was used as it contained about 25% of the total number of genes. Most of the genes fell in between 70 - 130% of closely expressed LGG and GBM to control.

A total of 35 different genes were then identified and further investigated in USCS Xena. Using analysis from Xena browser, the p value of Kaplan Meier plot and the F value (one-way anova) comparing GTEX, LGG and GBM. These values of the genes

were plotted on a scatter plot graph. The P value was plotted on a log scale which excluded 5 genes.

2.8 Statistics

Excel was used to analyse the raw data from USCS Xena browser to filter the genes down to a respectable number to be further investigated, Prism 9 and Image J were programmes used for statistical test. Prism 9 was used for every experimental analysis for bioinformatics, treatment, and ELISA. One way and two-way anova stats was performed, relevant post-hoc such as Tukey test. P value at < 0.05 was deemed significant. To quantify *BRCA2* image J was used.

2.9 Western blot

All Consumable was bought from Thermo scientific unless said otherwise. The composition of buffers used are found in appendix 4.

Imaging of the membranes was done using Biorad ChemiDOC Imaging system.

2.9.1 Method development – Amyloid beta quantification

Initial attempts to separate amyloid beta from the cell lysates were by SDS-PAGE and western blotting. Various gels were freshly made in house to try and successfully quantify the protein.

The composition of all gels contained 2.5M tris buffer (pH 8.8) and 29:1 Acrylamide/ bis-acrylamide. The stacking gel was always 4% and separating gel (if used) was 10%. The resolver gel was 16 %. 6M Urea was sometimes added to the resolver gel. A tricine sample buffer was used for loading. Running buffer used was a tris-tricine buffer. Gels were run at 150v for 90 mins. Tris-glycine was used as the transfer buffer. During transfer an ice block was used to counter overheating and the protein was transferred to a PVDF or nitrocellulose membrane, at 300mA for 80 minutes.

A 10% tricine SDS PAGE gel (4% stacking gel) were made for the detection of *BRCA2*. The composition of the gels contained 2.5M tris buffer (pH 8.8) and 29:1 Acrylamide/ bis-acrylamide. A tricine sample buffer was used for loading. Running buffer used was a tris-tricine buffer. Tris-glycine was used as the transfer buffer. Gels were run at 100v for 120 mins or until the relevant bands are ran off the gel. During transfer an ice block was used to counter overheating and the protein was transferred to a PVDF membrane, under the conditions of 300mA for 80 mins.

CHAPTER 3

RESULTS

3.1 Quantification of A β 40 and A β 42 by western blot and ELISA

Western Blot

The antibodies used for staining were tested on a dot blot experiment to make sure they are viable to use (appendix, image 1.1, 1.2). Ponceau S stain was done to show transfer of proteins from gel to membrane (appendix 1, Image 1.3).

The first gel run comprised of 4% stacking and 16% resolving gel. The gel was run for 90 mins at 150v in running buffer (tris, tricine, SDS) and a Tris-sample buffer was used for loading. The gel was transferred on a Cellulose membrane at 300mA for 80 mins (Image 3.1, 3.2). In this run, the proteins did not run through the stacking gel to the resolving gel which I believe was due to the jump in from 4% to 16%. Due to this, a separating gel was used in other to facilitate movement from stacking gel to resolving gel.

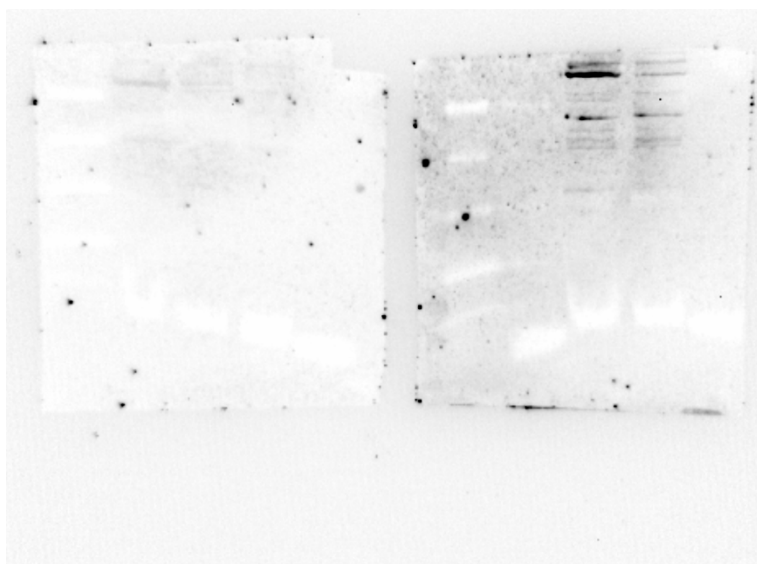


Image 3.1; 16% gel, A β 40 stain on left and A β 42 stain on right, lanes from left to right, ladder, 1321N1, U-87MG, SVGp12 and sample buffer

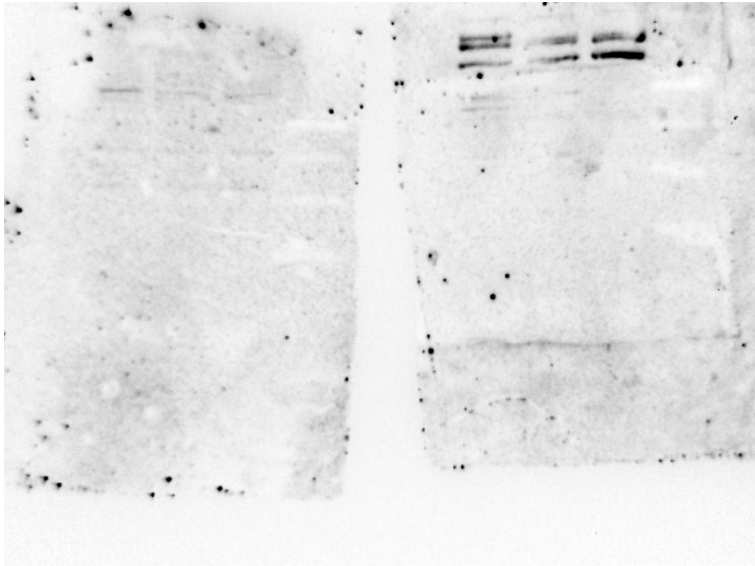


Image 3.2; 16 % gel, A β 40 stain on left and A β 42 stain on right, lanes from left to right, ladder, 1321N1, U-87MG, SVGp12 and sample buffer

In the second run, a 10% Image 3.3, Image 3.4). The gradient gel did not show any protein bands in the stacking gel which meant the proteins had travelled through the gel but unfortunately there were no bands in the entirety.

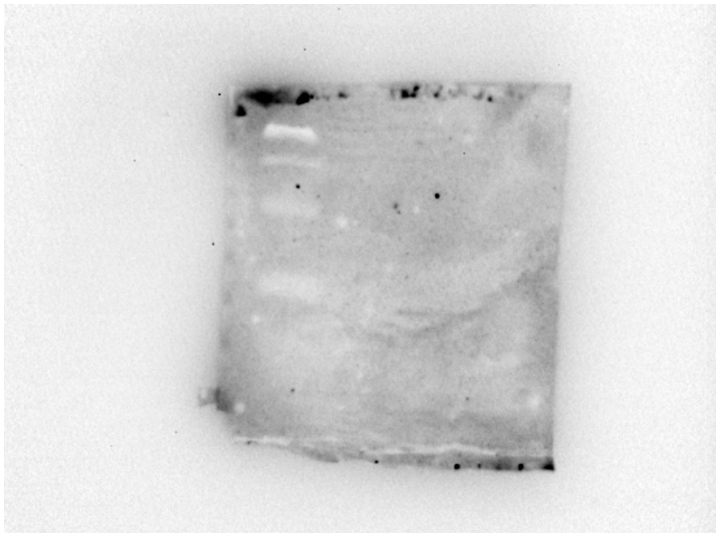


Image 3.3; Gradient gel, A β 40 stain, lanes from left to right, ladder, 1321N1, U-87MG, SVGp12 and sample buffer



Image 3.4; Gradient gel, A β 42 stain, lanes from left to right, ladder, 1321N1, U-87MG, SVGp12 and sample buffer

Due to the lack of bands, Urea was added to the Resolving gel in accordance with literature, as previous Western blot in which A β 40 and A β 42 was visualised, Urea was used. Everything else was kept the same. As seen in Image 3.5, 3.6 this did not yield any visible bands.

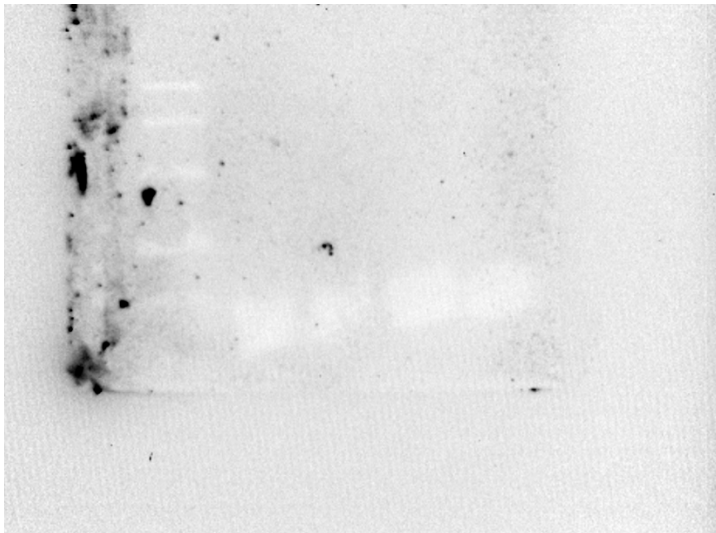


Image 3.5; Gradient gel (6M urea), A β 40 stain, lanes from left to right, ladder, 1321N1, U-87MG, SVGp12 and sample buffer

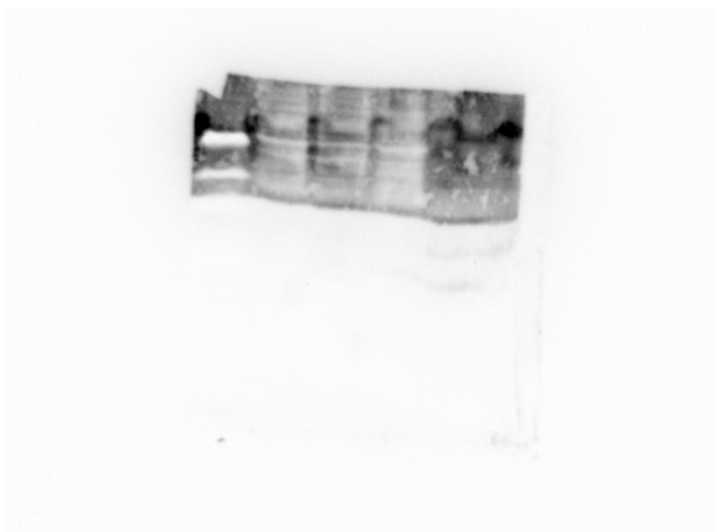


Image 3.6; Gradient gel (6m urea), A β 42 stain, lanes from left to right, ladder, 1321N1, U-87MG, SVGp12 and sample buffer.

The cellulose membrane was then changed to a PVDF membrane (Image 3.7, 3.8), even though nitrocellulose membrane is preferred for smaller molecular weight it is more brittle and fragile. All other conditions and components were kept the same. The results were still the same. Unfortunately, time ran out on figuring the limiting factor.

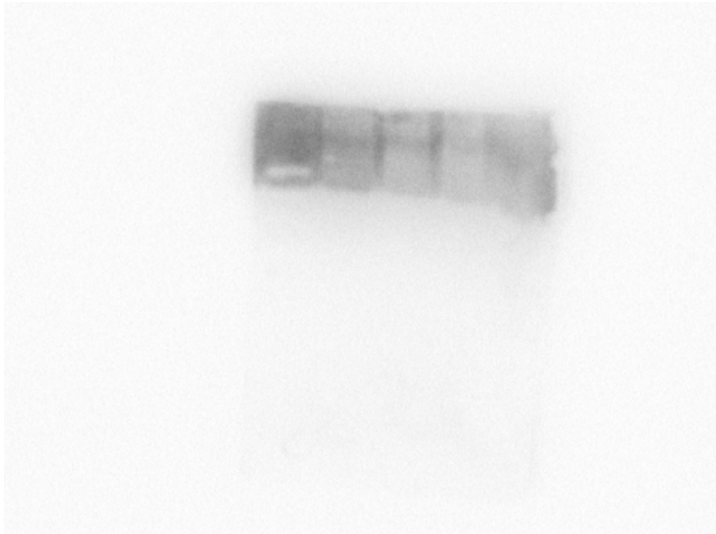


Image 3.7; Gradient gel, A β 40 stain, lanes from left to right, ladder, 1321N1, U-87MG, SVGp12 and sample buffer on PVDF membrane

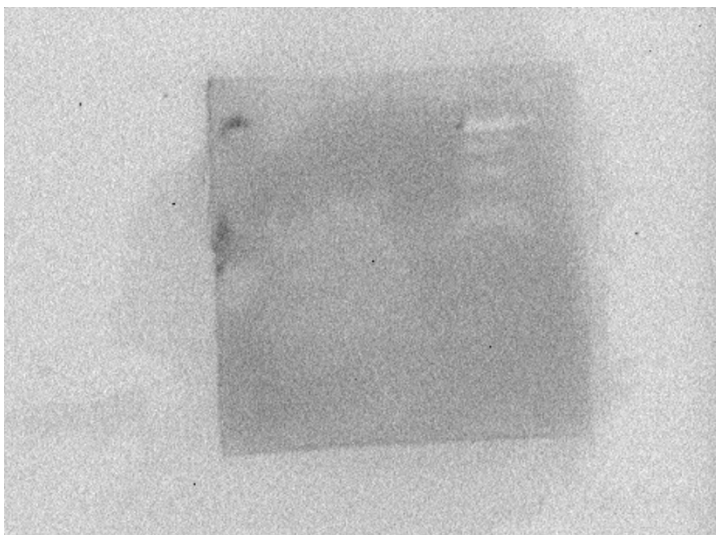


Image 3.8; Gradient gel, A β 42 stain, lanes from left to right, ladder, 1321N1, U-87MG, SVGp12 and sample buffer on PVDF membrane.

Stacking (%)	Separating (%)	Resolving (%)	Running conditions	Transfer conditions	Example image
4		16	Running buffer (tris, tricine, sds) – 90mins at 150v Sample buffer – tris sample buffer	Transfer - Cellulose membrane at 300mA for 80mins	Image 3.1 Image 3.2

4	10	16	Running buffer (tris, tricine, sds) – 90mins at 150v Sample buffer – tris sample buffer	Transfer - Cellulose membrane at 300mA for 80mins	Image 3.3 Image 3.4
4	10	16 (6m urea)	Running buffer (tris, tricine, sds) – 90mins at 150v Sample buffer – tris sample buffer	Transfer - Cellulose membrane at 300mA	Image 3.5, 3.6
4		16 (6m urea)	Running buffer (tris, tricine, sds) – 90mins at 150v Sample buffer – tris sample buffer	Transfer – PVDF membrane at 300mA for 40mins	Image 3.7, 3.8

Table 1: Gel and running conditions trialed for quantification of ab40 and ab42 by western blot

3.1.1 ELISA

Quantification of Ab40 and Ab42 in cell lysates was performed by ELISA. No differences in mean protein levels between the three cell lines were detected (Figure 1, $p > 0.05$, one-way ANOVA $n=3$). It was noted that there was variability between the three different passages for each cell line, despite being quantified in triplicate. However, no statistical difference was seen between the three different passages for each cell line (Appendix 1, $p > 0.05$, one way ANOVA, $n=3$) a trend towards increased expression in later passages was observed.

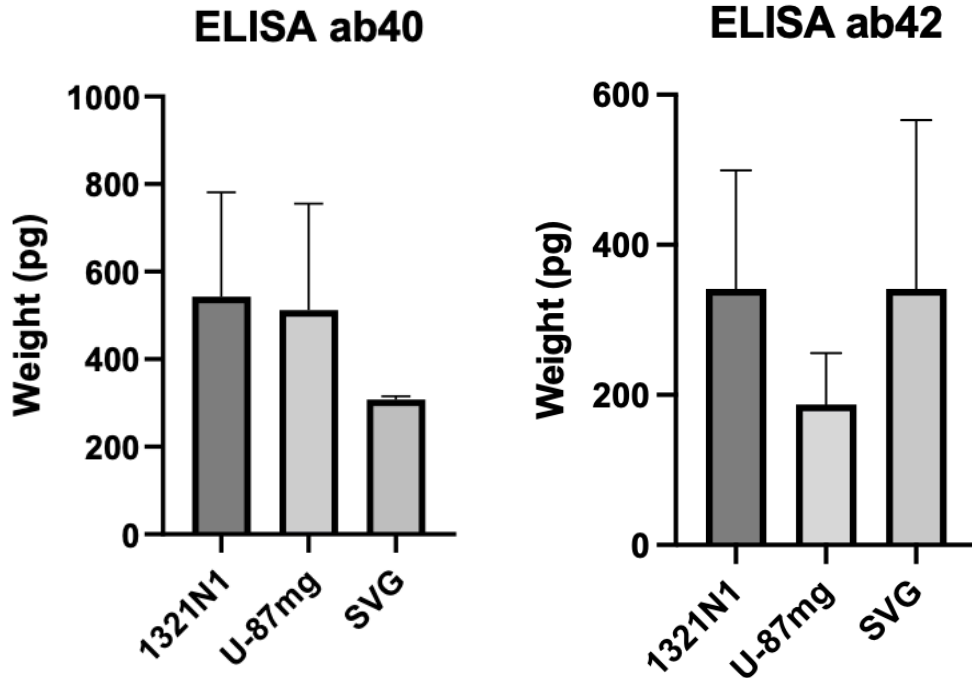
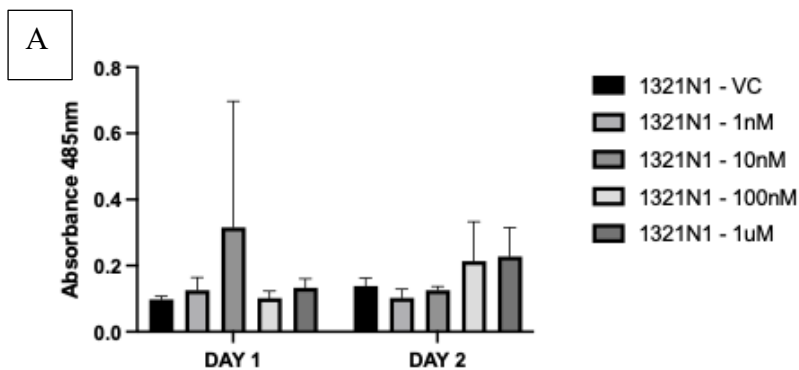


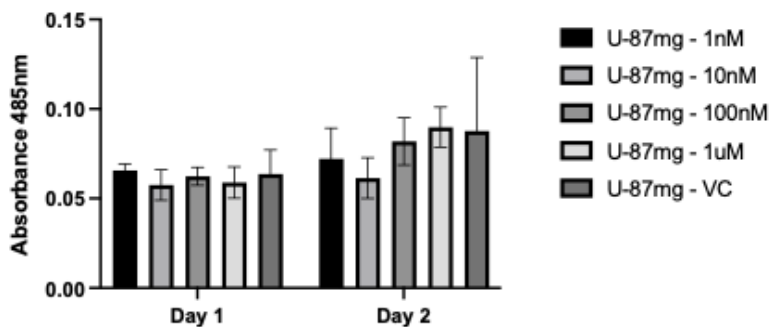
Figure 3.1; Mean amyloid expression for Ab40 (A) and Ab42 (B) in cell lysates from 1321N1, U-87mg and SVGP12 cell lines. No differences in mean expression were detected between the different cell types ($p > 0.05$, one way ANOVA, $n=3$).

3.2 Effect of amyloid inhibition on glioma cell growth

β -amyloid inhibitor optimisation was performed using a CCK-8 assay to assess cell viability after a day or 2 of exposure to the amyloid inhibitor at varying concentrations. No difference in mean absorbance was seen between the different inhibitor concentrations and vehicle control (VC) for all three cell lines 1321N1, U-87MG and SVGP12 (Figure 2.1, $P > 0.05$, one way ANOVA, $n=3$).



B



C

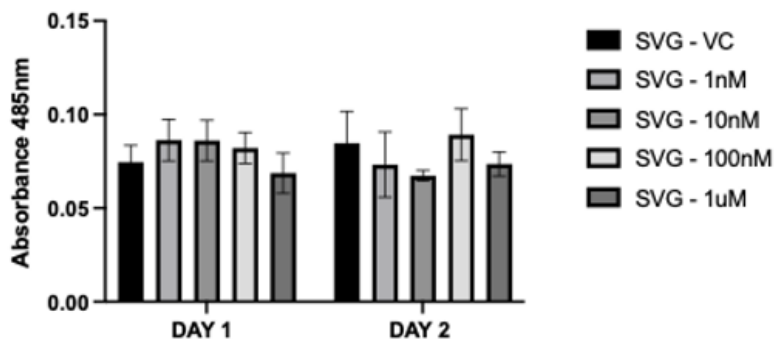


Figure 3.2; β -amyloid inhibitor optimisation for (A) 1321N1, (B) U-87mg and (C) SVGp12 cell lines. No differences in inhibitor concentration on growth were detected between the different cell types ($p > 0.05$, one way ANOVA, $n=3$).

As no effect on cell viability was seen on exposure to amyloid inhibitor over two days, viability was then determined over 7 days. A concentration of 100nM β -amyloid inhibitor was used in accordance with literature (Hong et al., 2010).

The three cell types 1321N1, U-87MG and SVGp12 were treated with 100 nM β -amyloid inhibitor for 7 days. The cell count was performed using a CCK-8 assay. No difference in mean absorbance was seen between treated and untreated cells for all three cell types (Figure 2.2, $P > 0.05$, one way ANOVA, $n=3$). U-87 and 1321N1 cells displayed normal growth however the growth of SVGp12 was very inconsistent and unreliable.

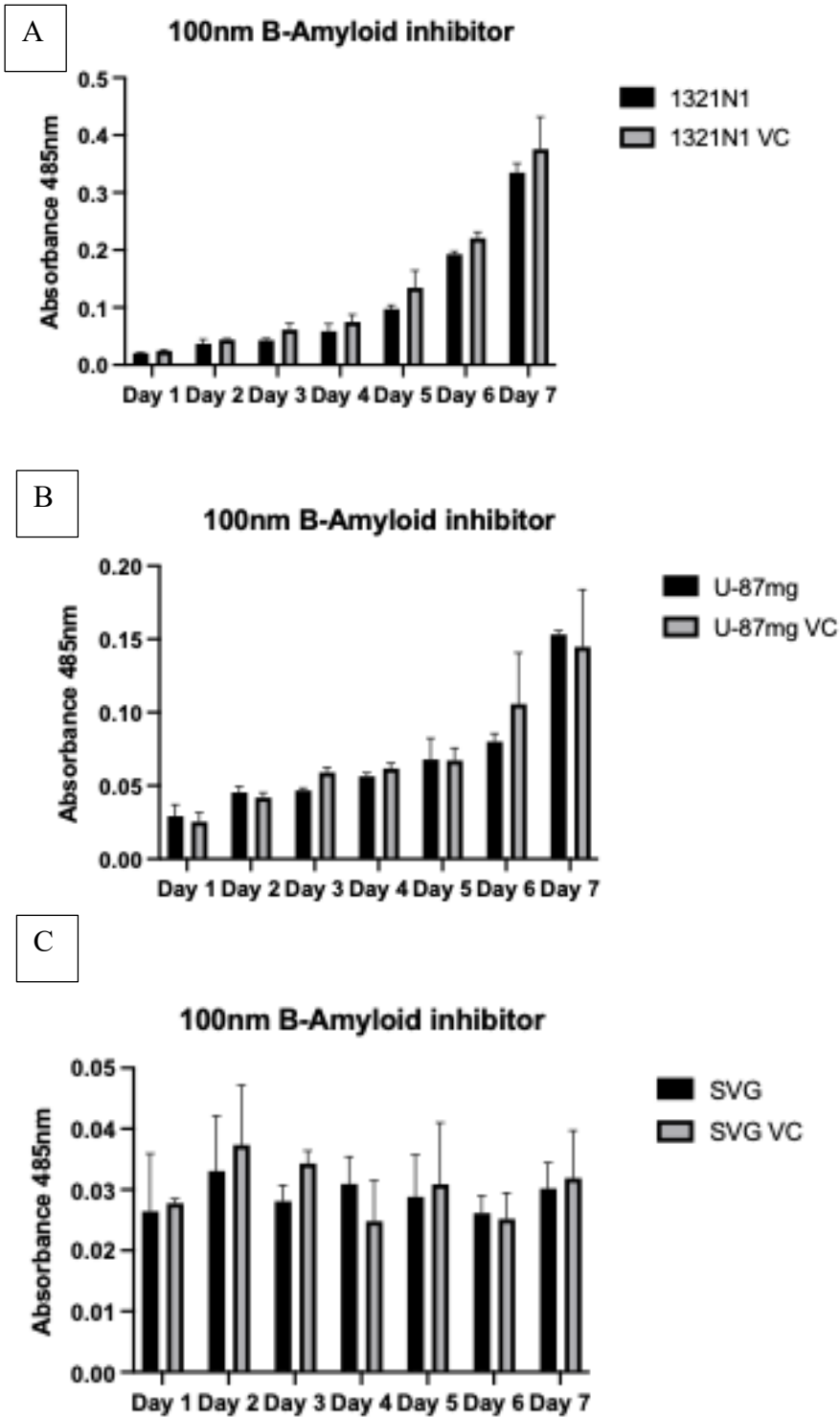


Figure 3.2.1; Cells treated with 100 nm β -amyloid inhibitor (A) 1321N1, (B)U-87mg and (C) SVGp12 cell lines. No differences of treated cells the different cell types ($p>0.05$, one way ANOVA, $n=3$)

3.3 Bioinformatic exploration of amyloid associated proteins

The top 30 genes linked to amyloid from (appendix 19) were taken forward for data extraction. The TCGA TARGET GTEx dataset on Xena ((UCSC Xena, n.d.) were limited to brain as primary site and main category to GTEx, TCGA low grade glioma and TCGA glioblastoma which yielded 1825 samples. Gene expression RNA-seq ($\log_2(\text{norm_count}+1)$) for each identified gene in GBM, LGG and normal tissue was compared in Xena and is available at xenabrowser.net.

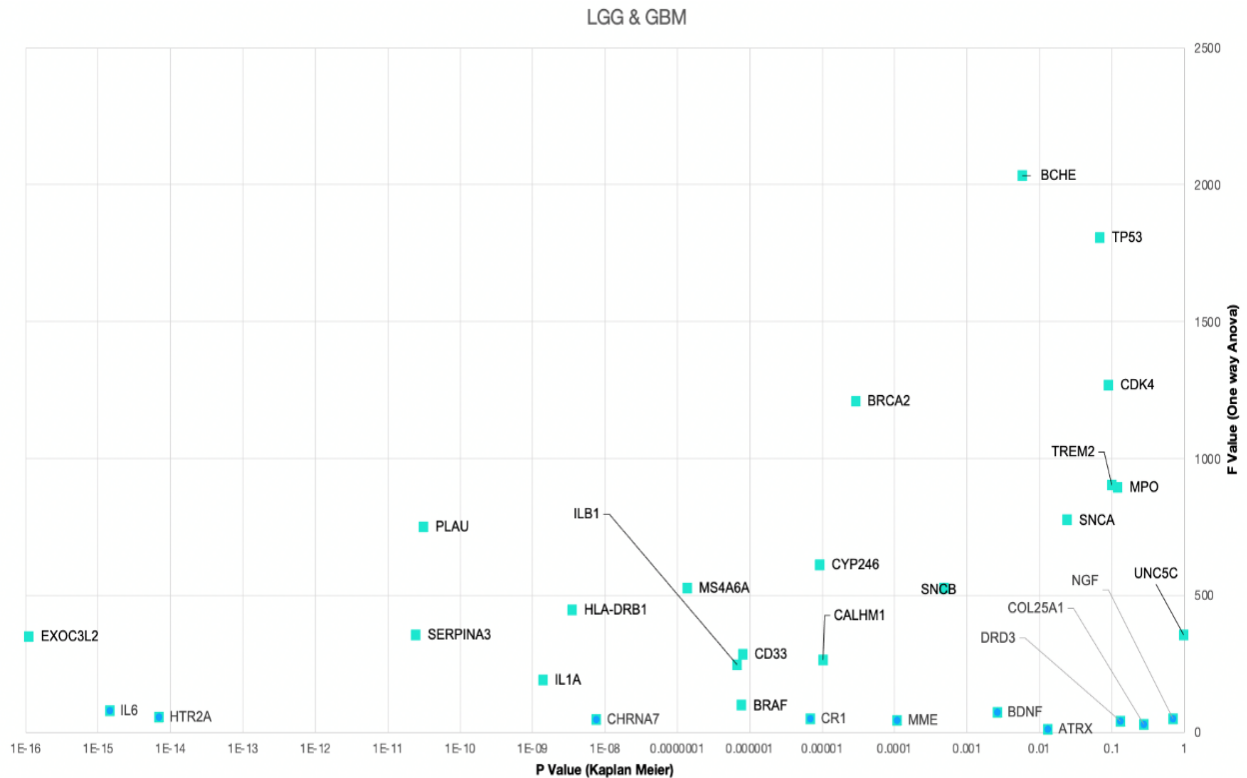


Figure 3.3; Total of 30 genes expressed in LGG and GBM P value (Kaplan Meier) and F value of one-way anova

Kaplan-Meier analysis was undertaken for each gene and p values extracted. As KM survival data only includes LGG and GBM patients, this would potentially exclude a gene whose expression was changed in both GBM and LGG and was different to normal tissue. Consequently, the f values were also extracted when GBM, LGG and normal tissue groups were compared to give an indication of spread of the three groups. Plotting p value against f value revealed a distribution that enabled identification of genes that had high f values and low p values. Four genes (*BCHE*, *TP53*, *CDK4* and *BRCA2*) had an f value greater than of a 1000 indicating the greatest disparity between GBM, LGG and normal tissue. Of those, *BRCA2* had the lowest p value indicating greatest distinction between high and low expression. This and a P value of less than 0.0001. In addition to *BRCA2*, *BCHE* also had a F value greater than 1000 and p value < 0.01. Unlike *BRCA2*, *BCHE* is a susceptibility gene of AD.

3.3.1 Expression of *BRCA2* in glioma

Analysis of raw RNA-seq data revealed significantly higher expression of *BRCA2* in GBM and LGG than in control tissue (Figure 3.5 $p < 0.05$ one-way ANOVA).

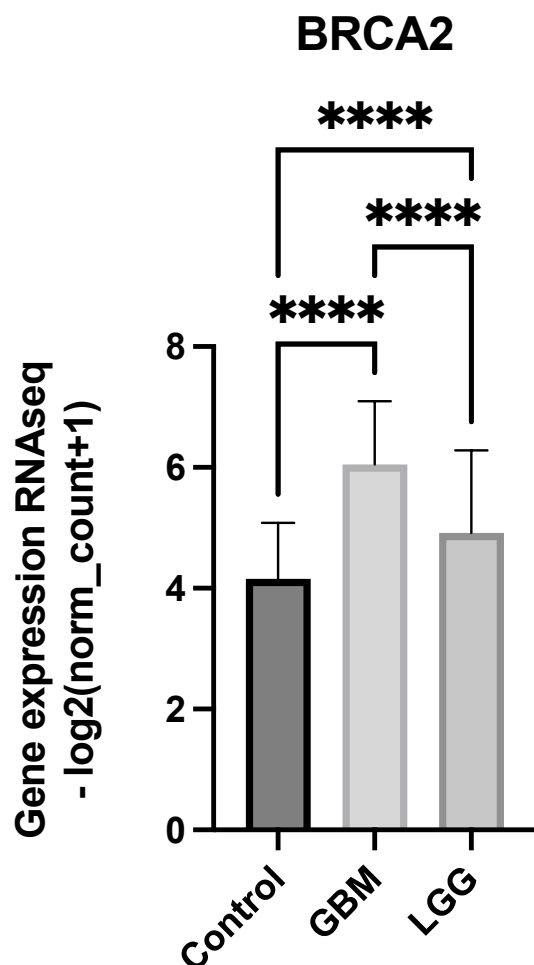


Figure 3.3.1; Mean *BRCA2* expression in GBM, LGG and normal tissue from TCGA, TARGET and GTex datasets. Increased expression was seen in both GBM and LGG compared to control tissue ($p < 0.05$ one-way ANOVA).

Kaplan Meier survival analysis of GBM and LGG datasets compared survival in two groups higher and lower than median expression. There were 51 samples from patients that had expression greater than the median, whereas 635 samples had expression less than the median. High expression of *BRCA2* was strongly associated with reduced survival (Figure 3.3.2, $p = 0.0000289$ log-rank test in Xenabrowser.net).

Kaplan Meier gene expression RNAseq - RSEM norm_count

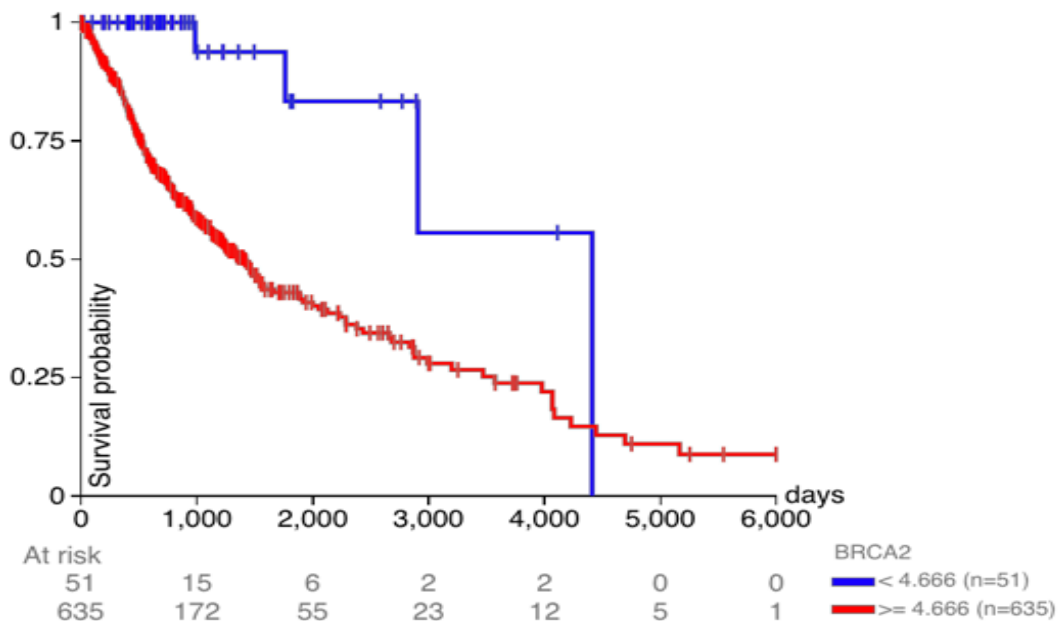


Figure 3.3.2; Kaplan-Meier survival analysis for overall survival relative to *BRCA2* expression (RNAseq-RSEM norm_count). High expression (red line) was strongly associated with reduced survival ($p=0.00002890$, Xenabrowser.net). Probing a western blot for *BRCA2* revealed a band at around 71 kDa in cell lysates from 1321N1 cells but very little in cell lysates from U-87 and SVGp12. *BRCA2* has a reported size of 390 kDa (Powell & Kachnic 2003). B-actin loading was comparable (Figure 3.3.3) and revealed a band at 41kDa as expected. Densitometric analysis confirmed significantly lower *BRCA2* protein in U87-mg and SVGp12 than 1321N1 cell lysates (Figure 3.3.3 $p<0.05$, one-way ANOVA, $n=3$).

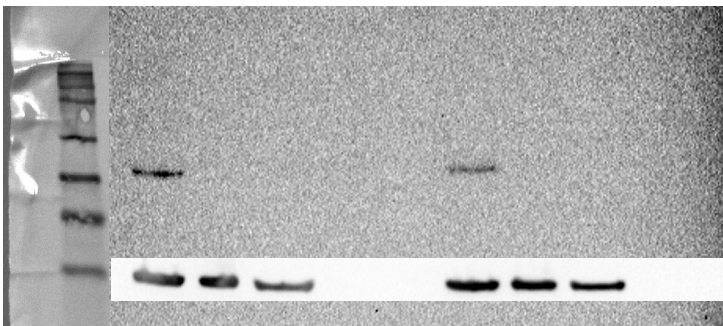


Image 3.9; Representative western blot of cell lysates probed for *BRCA2*. Lanes were loaded from L-R: ladder, 1321N1, U87-mg, SVGp12, sample buffer, ladder, 1321N1, U87-mg, SVGp12. B-actin was used as loading control.

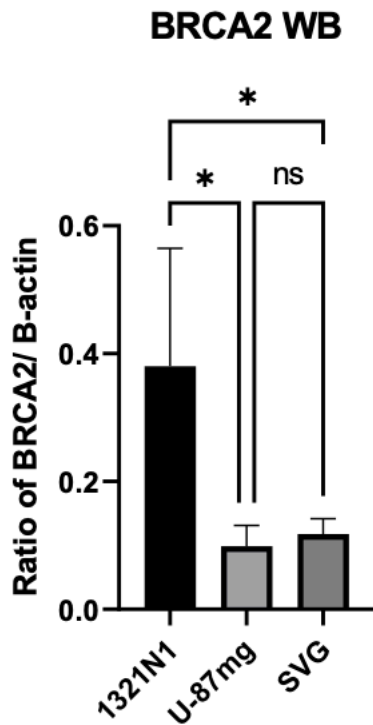


Figure 3.3.4; Densitometric analysis of western blot BRCA2 staining. Analysis of mean ratio of BRCA2/ β -actin staining showed less BRCA2 in U-87 and SVGp12 compared to 1321N1 ($p < 0.05$, one-way ANOVA, $n = 3$).

3.3.2 Expression of BCHE in glioma

and
and
lower

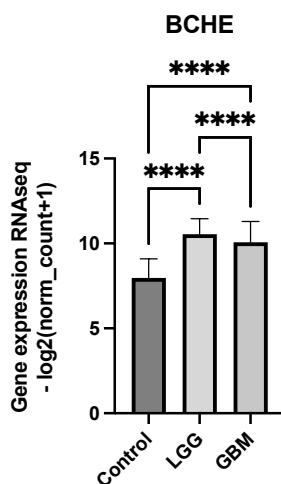


Figure 3.3.5; Mean BCHE expression in GBM, LGG normal tissue from TCGA, TARGET and GTex datasets. Increased expression was seen in both GBM LGG compared to control tissue ($p < 0.05$ one-way ANOVA).

Kaplan Meier survival analysis of GBM and LGG datasets compared survival in two groups higher and than median expression. There were 22 samples from patients that had expression greater than the median, whereas 664 samples had expression less than the median. High expression of BCHE was strongly associated with reduced survival (Figure 3.3.6, $p = 0.005855$ log-rank test in Xenabrowser.net).

Kaplan Meier gene expression RNAseq - RSEM norm_count

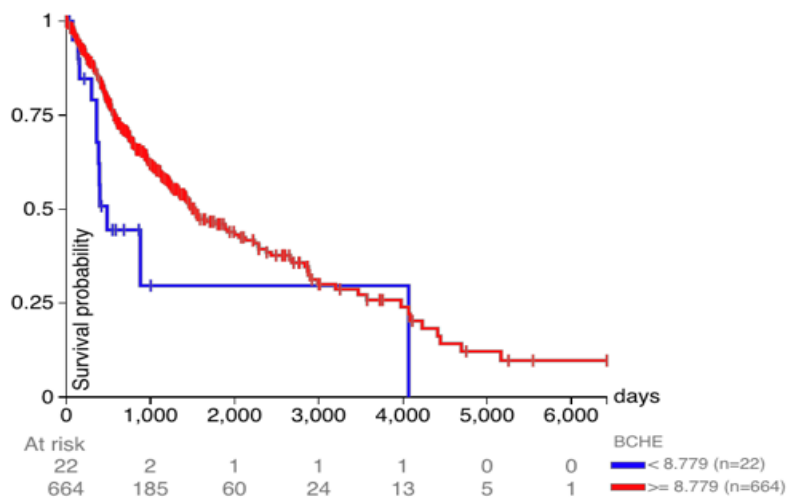


Figure 3.3.6. Kaplan-Meier survival analysis for overall survival relative to BCHE expression (RNAseq-RSEM norm_count). High expression (red line) was strongly associated with reduced survival ($p= 0.005855$, Xenabrowser.net).

CHAPTER 4

DISCUSSION

4.1 Amyloid beta as putative target in glioblastoma

The primary objective was to quantify A β 40 and A β 42 in glioblastoma cell lines. While western blotting did not achieve this goal, ELISA was successful and suggested no difference in cell content between high grade, low grade and control astrocytes. Exposure to the amyloid inhibitor K01-162 for 7 days had no effect on cell viability.

Previous studies have considered the role of β -amyloids in glioma and demonstrated amyloid accumulation in U87 cells (Li et al. 2014) and in tissue (Kucheryavykh et al 2019). Although the nature of A β in glioblastoma remains unclear, Paris and colleagues (2010) showed 40 – 50% tumour suppression following implantation of GBM cells into brain of transgenic mouse that overexpress A β compared to wild-type mice. In addition, Zhao et al (2009) reported reduced rate of proliferation of U-87MG when in presence of conditioned media from APP overexpressing cell suggesting increased production and protection from amyloid.

Expression levels of A β 40 and A β 42 as determined by ELISA suggested similar levels across cell lines. It may be that relative variation between amyloid isoforms is the driving factor. Ordinarily A β 40 accounts for 80 - 90% of ABO with A β 42 accounting for 5 – 10% (Murphy and LeVine, 2010) however in FAD a decrease in ratio of A β 40 / A β 42 has been linked to an increase in FAD mutations (Arber et al., 2020). Our data suggests a decrease in ratio of A β 40 / A β 42 which would agree with the initial hypothesis that Alzheimers is protective against cancer. Ibanez et al (2014) proposed CNS and cancer share or express common genes/ pathways in opposite directions therefore supporting the inverse comorbidity seen. If this is the case, the decrease in ratio of A β 40 / A β 42 in glioblastoma should mean a better prognosis.

Data presented here suggests expression of amyloid is similar between high grade, low grade and control glial cell lines. Consequently, targeting amyloid may not be a useful strategy in treating GBM. Pharmacological inhibition of amyloid has been an active strategy against Alzheimer's disease for many years and multiple drugs have been developed and recently showed promise in the clinic (reviewed by Zhang et al 2023). That we were unable to see any effects here may initially be due to our choice of drug. K162 inhibits the aggregation of A β and prevents the formation of amyloid oligomers (Mrdenovic et al 2021) however it is not clear if the A β detected by ELISA is in monomeric, dimeric or oligomeric forms. In addition, as we saw no significant difference between amyloid expression in lysates from the three cell lines, it may be that they are all being inhibited similarly or that any oligomerisation could already have occurred prior to the K162 inhibitor being applied as oligomerisation can occur within minutes (Cline et al. 2018). Moreover, the result of the A β could have been due to the optimisation stage, as the treatment was introduced to cells immediately after seeding during the lag phase and the optimisation was only done for two days. This could have resulted in choosing a concentration for the treatment. Of note however, K162 is one of the most potent amyloid inhibitors and the concentration of 100 nM applied here is in line with the reported EC50 of 0.080 μ M (Li et al 2011). K01-162 is a fluorene compound that binds directly to β -amyloid oligomer (ABO) inhibiting its subsequent binding to synapses (Hong et al., 2010). The compounds

high affinity to ABO is shown by its dissociation constant (K_d) of 19 μM so either there is no amyloid present to inhibit formation, the fibrils had already formed or the presence or lack of amyloid has no bearing on cell viability.

Although direct inhibition of $\text{A}\beta$ oligomerisation was unsuccessful here, that may suggest that targeting $\text{A}\beta$ associated proteins in the amyloid pathway may be a worthwhile alternative. The amyloid precursor is cleaved by β -secretase (BACE) to CTF before cleavage by γ -secretase to $\text{A}\beta$. BACE1 inhibition has recently been shown to suppress GBM growth in an in vivo xenograft model (Zhai et al 2021) by a novel mechanism suppressing macrophage phagocytosis of tumour cells rather than by interfering with the amyloid cascade. The authors however did not consider amyloid per se, so a simultaneous effect on $\text{A}\beta$ cannot be ruled out.

4.2 Technical consideration of $\text{A}\beta_{40}$ and $\text{A}\beta_{42}$ quantification

The initial aim of the project was to quantify amyloid isoforms in cell lysates. Western blotting is one of the standard techniques to determine protein expression and is routinely applied in our lab. Consequently, it seemed a reasonable starting place towards the first objective.

Despite being the subject of studies regarding Alzheimer's disease for many years, amyloid quantification by western blot is possible, but not widely reported in the literature. Amyloid quantification in glioma cell lysates has not been reported. Some prominent papers that guided early studies were summarised in section 1.6.

After trying numerous methodologies, the main point drawn from the literature was that inclusion of urea in the gel is vital for the separation of the smaller proteins. Urea is a more powerful de-naturant than SDS, however electrophoretic properties can differ from SDS-PAGE. The concentration of urea chosen here was in line with previously reported methodologies and did not yield any separation of amyloid. Consequently, attention turned to the other electrophoresis components.

A common alternative for electrophoresis of small molecular weight proteins is tris-tricine gel. Replacing glycine with tricine favours small protein separation as larger proteins are destacked so enter the separating gel later (Schagger and von Jagow 1987). This is possible as tricine has greater negative charge and higher ionic strength than glycine, so proteins are more attracted to the anode. Alongside the tricine gel, a tricine running buffer was also trialled. This appeared to work successfully as the small molecular weight (mw) ladder was resolved appropriately.

Consequently, it seems likely that the inability to resolve and probe for low molecular weight proteins may arise at the transfer stage. Though the result of Ponceau S showed transfer of proteins from the gel to the membrane, it did not confirm whether ABO was transferred on to the membrane or to a lesser point whether ABO passed through the membrane as the protein is small. PVDA was chosen in latter trials as it has greater protein binding capacity than the nitrocellulose membranes tried originally. Pass through the membrane of low molecular weight proteins is also possible and is determined by pore size with standard membrane pore size being

0.45µm. Alternative pore sizes weren't excluded during trials here, so it may be possible that using a 0.2µm or 0.1µm pore membrane would be more successful. Similarly, transfer conditions can be varied to reduce the likelihood of overtransfer and losing protein as it passes through the membrane. Duration of transfer was decreased to test the theory without success. Further work could have been undertaken to vary current conditions.

4.3 Bioinformatics

4.3.1 *BRCA2 and BCHE as new targets in glioblastoma*

The bioinformatic exploration identified *BRCA2* as a protein associated with amyloid that warranted further investigation. *BRCA* exists in two forms, *BRCA1* and *BRCA2* and is involved in DNA damage response and DNA repair. The protein is instrumental in homologous repair (HR) as the recruiter of *RAD51* which is responsible for the tumour suppressor aspect of HR (Roy et al., 2012). *BRCA1* mutations increase risk of breast cancer from approximately 13% to 55-72% while mutation in *BRCA2* increases risk to 45-69%. The importance of *BRCA2* in glioblastoma is less known but *RAD51* showed 51% elevation in GBM with an increase of 15 months compared to specimens with moderate or absent levels of *RAD51* with a survival of 9 months (Welsh et al 2009). Furthermore, *BRCA2* inhibits the cleavage of *RAD51* by caspase 3 following radiation (Brown et al., 2008). In TMZ resistant glioma cells the inhibition of *BRCA1*, *BRCA2* & *RAD51* increased the sensitivity of TMZ (Chai et al., 2014). The involvement of *BRCA* in cancers other than breast cancer has been extended to ovarian, fallopian tube and prostate. A link to GBM has previously been suggested for *BRCA1* (Boukerroucha et al. 2015) and has recently been suggested to be a prognostic biomarker with low expression correlating with more favourable outcomes (Vassiloukopalou et al 2021). Recently, interest has extended to *BRCA2* and data corroborating that presented here been published (Meimand et al 2021). Further study is needed to establish a role of *BRCA2* in GBM and its potential utility as therapeutic avenue, prognostic biomarker or biomarker to allow personalised treatment.

4.3.2 *BCHE*

The significance in RNAseq expression of *BCHE* in GBM and LGG in comparison to control is interesting as the gene or protein is not documented in glioma. Although, *BCHE* has been linked to tumorigenesis (Soreq et al., 1989; Bernardi et al., 2020). Moreover, reports linking *BCHE* to lung (Brass et al., 1997), prostate cancer (Gu et al 2018) and breast cancer (Bernardi et al., 2020) might open the door to further research in glioma especially after THOMSON and SONTHEIMER (2019) points to an increase expression of *ACh* receptors in glioma and subsequently have a role migration and the fact that *BCHE* is involved in the metabolism of *ACh* (Darvesh, 2016).

4.4 Conclusion

In this study I was able to quantify A β 40 and A β 42 in lysates from immortalised high grade GBM cells, low grade glioma cells and control astrocytes. No differences in expression were detected between the three cell types. The amyloid oligomerisation inhibitor K162 similarly showed no efficacy. BRCA2 and BCHE were identified as alternative targets by bioinformatics. BRCA2 showed significantly higher expression in low grade glioma cells than control astrocytes. The role of BRCA2 in glioma has not been previously considered and should be the subject of further research.

CHAPTER 5 REFERENCE

Ahmed, M., Davis, J., Aucoin, D., Sato, T., Ahuja, S., Aimoto, S., Elliott, J.I., Van Nostrand, W.E. and Smith, S.O., 2010. Structural conversion of neurotoxic amyloid- β 1–42 oligomers to fibrils. *Nature structural & molecular biology*, 17(5), pp.561-567.

Alzial, G., Renoult, O., Paris, F., Gratas, C., Clavreul, A. and Pecqueur, C., 2022. Wild-type isocitrate dehydrogenase under the spotlight in glioblastoma. *Oncogene*, 41(5), pp.613-621.

Arber, C., Toombs, J., Lovejoy, C., Ryan, N.S., Paterson, R.W., Willumsen, N., Gkanatsiou, E., Portelius, E., Blennow, K., Heslegrave, A. and Schott, J.M., 2020. Familial Alzheimer's disease patient-derived neurons reveal distinct mutation-specific effects on amyloid beta. *Molecular psychiatry*, 25(11), pp.2919-2931.

Bass, J.J., Wilkinson, D.J., Rankin, D., Phillips, B.E., Szewczyk, N.J., Smith, K. and Atherton, P.J., 2017. An overview of technical considerations for Western blotting applications to physiological research. *Scandinavian journal of medicine & science in sports*, 27(1), pp.4-25.

Bernardi, C.C., de SF Ribeiro, E., Cavalli, I.J., Chautard-Freire-Maia, E.A. and Souza, R.L., 2010. Amplification and deletion of the ACHE and BCHE cholinesterase genes in sporadic breast cancer. *Cancer genetics and cytogenetics*, 197(2), pp.158-165.

Binda, O., 2019. Chromatin Signaling and Neurological Disorders (Vol. 12). Academic Press.

Boukerroucha, M., Josse, C., Segers, K., El-Guendi, S., Frères, P., Jerusalem, G. and Bours, V., 2015. BRCA1 germline mutation and glioblastoma development: report of cases. *BMC cancer*, 15(1), pp.1-7.

Brass, N., Rácz, A., Heckel, D., Remberger, K., Sybrecht, G.W. and Meese, E.U., 1997. Amplification of the genes BCHE and SLC2A2 in 40% of squamous cell carcinoma of the lung. *Cancer research*, 57(11), pp.2290-2294.

Brown, E.T., Robinson-Benion, C. and Holt, J.T., 2008. Radiation enhances caspase 3 cleavage of Rad51 in BRCA2-defective cells. *Radiation research*, 169(5), pp.595-601.

Chai, K.M., Wang, C.Y., Liaw, H.J., Fang, K.M., Yang, C.S. and Tzeng, S.F., 2014. Downregulation of BRCA1-BRCA2-containing complex subunit 3 sensitizes glioma cells to temozolomide. *Oncotarget*, 5(21), p.10901.

Colovic, M.B., Krstic, D.Z., Lazarevic-Pasti, T.D., Bondzic, A.M. and Vasic, V.M., 2013. Acetylcholinesterase inhibitors: pharmacology and toxicology. *Current neuropharmacology*, 11(3), pp.315-335

COUZIN-FRANKEL, J. (2023). *Will unpredictable side effects dim the promise of new Alzheimer's drugs?* [online] Science.org. Available at: <https://www.science.org/content/article/will-unpredictable-side-effects-dim-promise-new-alzheimer-s-drugs> [Accessed Dec. 11AD].

Cui, H., King, A.E., Jacobson, G.A. and Small, D.H., 2017. Peripheral treatment with enoxaparin exacerbates amyloid plaque pathology in Tg2576 mice. *Journal of neuroscience research*, 95(4), pp.992-999.

Cummings, J., Lee, G., Ritter, A., Sabbagh, M. and Zhong, K., 2020. Alzheimer's disease drug development pipeline: 2020. *Alzheimer's & Dementia: Translational Research & Clinical Interventions*, 6(1), p.e12050.

Darvesh, S., 2016. Butyrylcholinesterase as a diagnostic and therapeutic target for Alzheimer's disease. *Current Alzheimer Research*, 13(10), pp.1173-1177.

Database, G., 2022. *beta amyloid related genes - GeneCards Search Results*. [online] Genecards.org. Available at: <<https://www.genecards.org/Search/Keyword?queryString=beta%20amyloid>> [Accessed 17 August 2022].

Forlenza, O.V., Spink, J.M., Dayanandan, R., Anderton, B.H., Olesen, O.F. and Lovestone, S., 2000. Muscarinic agonists reduce tau phosphorylation in non-neuronal cells via GSK-3 β inhibition and in neurons. *Journal of neural transmission*, 107(10), pp.1

Francis, P.T., Palmer, A.M., Snape, M. and Wilcock, G.K., 1999. The cholinergic hypothesis of Alzheimer's disease: a review of progress. *Journal of Neurology, Neurosurgery & Psychiatry*, 66(2), pp.137-147.

Gilard, V., Tebani, A., Dabaj, I., Laquerrière, A., Fontanilles, M., Derrey, S., Marret, S. and Bekri, S., 2021. Diagnosis and management of glioblastoma: A comprehensive perspective. *Journal of Personalized Medicine*, 11(4), p.258.

Glennner, G.G. and Wong, C.W., 1984. Alzheimer's disease: initial report of the purification and characterization of a novel cerebrovascular amyloid protein. *Biochemical and biophysical research communications*, 120(3), pp.885-890.

Gu, Y., Chow, M.J., Kapoor, A., Mei, W., Jiang, Y., Yan, J., De Melo, J., Seliman, M., Yang, H., Cutz, J.C. and Bonert, M., 2018. Biphasic alteration of butyrylcholinesterase (BChE) during prostate cancer development. *Translational oncology*, 11(4), pp.1012-1022.

Grech, N., Dalli, T., Mizzi, S., Meilak, L., Calleja, N. and Zrinzo, A., 2020. Rising incidence of glioblastoma multiforme in a well-defined population. *Cureus*, 12(5).

Haider, S.R., Reid, H.J. and Sharp, B.L., 2012. Tricine-sds-page. *Protein electrophoresis: methods and protocols*, pp.81-91.

Harman, D., 2006. Alzheimer's disease pathogenesis: role of aging. *Annals of the New York Academy of Sciences*, 1067(1), pp.454-460.

Hardy, J.A. and Higgins, G.A., 1992. Alzheimer's disease: the amyloid cascade hypothesis. *Science*, 256(5054), pp.184-186.

Haring, R., Gurwitz, D., Barg, J., Pinkaskramarski, R., Heldman, E., Pittel, Z., Wengier, A., Meshulam, H., Marciano, D., Karton, Y. and Fisher, A., 1994. Amyloid precursor protein secretion via muscarinic receptors: reduced desensitization using the M1-selective agonist AF102B. *Biochemical and biophysical research communications*, 203(1), pp.652-658.

Harman, D., 2006. Alzheimer's disease pathogenesis: role of aging. *Annals of the New York Academy of Sciences*, 1067(1), pp.454-460.

Hippius, H. and Neundörfer, G., 2003. The discovery of Alzheimer's disease. *Dialogues in clinical neuroscience*, 5(1), p.101.

Holtzman, D.M., Morris, J.C. and Goate, A.M., 2011. Alzheimer's disease: the challenge of the second century. *Science translational medicine*, 3(77), pp.77sr1-77sr1.

Hong, H.S., Maezawa, I., Budamagunta, M., Rana, S., Shi, A., Vassar, R., Liu, R., Lam, K.S., Cheng, R.H., Hua, D.H. and Voss, J.C., 2010. Candidate anti-A β fluorene compounds selected from analogs of amyloid imaging agents. *Neurobiology of aging*, 31(10), pp.1690-1699.

Hoogmartens, J., Cacace, R. and Van Broeckhoven, C., 2021. Insight into the genetic etiology of Alzheimer's disease: A comprehensive review of the role of rare variants. *Alzheimer's & Dementia: Diagnosis, Assessment & Disease Monitoring*, 13(1), p.e12155.

J Alzheimers Dis. 2018; 64(Suppl 1): S567–S610. Published online 2018 Jun 12. Prepublished online 2018 May 18. doi: 10.3233/JAD-179941 PMID: 29843241 The Amyloid- β Oligomer Hypothesis: Beginning of the Third Decade Erika N. Cline, Máira Assunção Bicca, Kirsten L. Viola, and William L. Klein*

Jiang, S., Li, Y., Zhang, C., Zhao, Y., Bu, G., Xu, H. and Zhang, Y.W., 2014. M1 muscarinic acetylcholine receptor in Alzheimer's disease. *Neuroscience bulletin*, 30(2), pp.295-307.

Kimura, N., Yanagisawa, K., Terao, K., Ono, F., Sakakibara, I., Ishii, Y., Kyuwa, S. and Yoshikawa, Y., 2005. Age-related changes of intracellular A β in cynomolgus monkey brains. *Neuropathology and applied neurobiology*, 31(2), pp.170-180.

Kish, S.J., Robitaille, Y., El-Awar, M., Schut, L., DiStefano, L., Ball, M.J. and Mazurek, M.F., 1993. Reduced cerebral cortical but elevated striatal concentration of somatostatin-like immunoreactivity in dominantly inherited olivopontocerebellar atrophy. *Journal of Neurology, Neurosurgery & Psychiatry*, 56(9), pp.1013-1015.

Kitagishi, Y., Nakanishi, A., Ogura, Y. and Matsuda, S., 2014. Dietary regulation of PI3K/AKT/GSK-3 β pathway in Alzheimer's disease. *Alzheimer's research & therapy*, 6(3), pp.1-7.

Klafki, H.W., Wiltfang, J. and Staufienbiel, M., 1996. Electrophoretic separation of β A4 peptides (1–40) and (1–42). *Analytical biochemistry*, 237(1), pp.24-29.

Konstantinidis, E., Molisak, A., Perrin, F., Streubel-Gallasch, L., Fayad, S., Kim, D.Y., Petri, K., Aryee, M.J., Aguilar, X., György, B. and Giedraitis, V., 2022. CRISPR-Cas9 treatment partially restores amyloid- β 42/40 in human fibroblasts with the Alzheimer's disease PSEN1 M146L mutation. *Molecular therapy-Nucleic acids*, 28, pp.450-461.

KoSIK, K.S., Joachim, C.L. and Selkoe, D.J., 1986. Microtubule-associated protein tau (tau) is a major antigenic component of paired helical filaments in Alzheimer disease. *Proceedings of the National Academy of Sciences*, 83(11), pp.4044-4048.

Kucheryavykh, L.Y., Ortiz-Rivera, J., Kucheryavykh, Y.V., Zayas-Santiago, A., Diaz-Garcia, A. and Inyushin, M.Y., 2019. Accumulation of innate amyloid beta peptide in glioblastoma tumors. *International journal of molecular sciences*, 20(10), p.2482.

Li, J., Liu, R., Lam, K.S., Jin, L.W. and Duan, Y., 2011. Alzheimer's disease drug candidates stabilize A- β protein native structure by interacting with the hydrophobic core. *Biophysical journal*, 100(4), pp.1076-1082.

Liu, J., Hlávka, J., Hillestad, R.J. and Mattke, S., 2020. Alzheimer's disease facts and figures. *Alzheimer's Dement*, 16, pp.391-460.

Long, H.Z., Cheng, Y., Zhou, Z.W., Luo, H.Y., Wen, D.D. and Gao, L.C., 2021. PI3K/AKT signal pathway: A target of natural products in the prevention and treatment of Alzheimer's disease and Parkinson's disease. *Frontiers in pharmacology*, 12, p.619.

Mandelkow, E., Von Bergen, M., Biernat, J. and Mandelkow, E.M., 2007. Structural principles of tau and the paired helical filaments of Alzheimer's disease. *Brain pathology*, 17(1), pp.83-90.

Mayeux, R. and Stern, Y., 2012. Epidemiology of Alzheimer disease. *Cold Spring Harbor perspectives in medicine*, 2(8), p.a006239.

Mazanetz, M.P. and Fischer, P.M., 2007. Untangling tau hyperphosphorylation in drug design for neurodegenerative diseases. *Nature reviews Drug discovery*, 6(6), pp.464-479.

McKinnon, C., Nandhabalan, M., Murray, S.A. and Plaha, P., 2021. Glioblastoma: clinical presentation, diagnosis, and management. *Bmj*, 374.

Medeiros, R., Baglietto-Vargas, D. and LaFerla, F.M., 2011. The role of tau in Alzheimer's disease and related disorders. *CNS neuroscience & therapeutics*, 17(5), pp.514-524.

Meimand, S.E., Pour-Rashidi, A., Shahrabak, M.M., Mohammadi, E., Meimand, F.E. and Rezaei, N., 2022. The prognostication potential of BRCA genes expression

in gliomas: a genetic survival analysis study. *World Neurosurgery*, 157, pp.e123-e128.

Mendes, C.T., Mury, F.B., de Sá Moreira, E., Alberto, F.L., Forlenza, O.V., Dias-Neto, E. and Gattaz, W.F., 2009. Lithium reduces Gsk3b mRNA levels: implications for Alzheimer disease. *European archives of psychiatry and clinical neuroscience*, 259(1), pp.16-22.

Miranda-Filho, A., Piñeros, M., Soerjomataram, I., Deltour, I. and Bray, F., 2017. Cancers of the brain and CNS: global patterns and trends in incidence. *Neuro-oncology*, 19(2), pp.270-280.

Mondesir, J., Willekens, C., Touat, M. and de Botton, S., 2016. IDH1 and IDH2 mutations as novel therapeutic targets: current perspectives. *Journal of blood medicine*, pp.171-180.

Mrdenovic, D., Zarzycki, P., Majewska, M., Pieta, I.S., Nowakowski, R., Kutner, W., Lipkowski, J. and Pieta, P., 2021. Inhibition of amyloid β -induced lipid membrane permeation and amyloid β aggregation by K162. *ACS chemical neuroscience*, 12(3), pp.531-541.

Noble, W., Planel, E., Zehr, C., Olm, V., Meyerson, J., Suleman, F., Gaynor, K., Wang, L., LaFrancois, J., Feinstein, B. and Burns, M., 2005. Inhibition of glycogen synthase kinase-3 by lithium correlates with reduced tauopathy and degeneration in vivo. *Proceedings of the National Academy of Sciences*, 102(19), pp.6990-6995.

Office for National Statistics (2021). *National life tables – life expectancy in the UK - Office for National Statistics*. [online] www.ons.gov.uk. Available at: <https://www.ons.gov.uk/peoplepopulationandcommunity/birthsdeathsandmarriages/lifeexpectancies/bulletins/nationallifetablesunitedkingdom/2018to2020>.

Paris, D., Patel, N., Ganey, N.J., Laporte, V., Quadros, A. and Mullan, M.J., 2010. Anti-Tumoral Activity of a Short Decapeptide Fragment of the Alzheimer's A β Peptide. *International journal of peptide research and therapeutics*, 16, pp.23-30.

Pagano, A., Breuzard, G., Parat, F., Tchoghandjian, A., Figarella-Branger, D., De Bessa, T.C., Garrouste, F., Douence, A., Barbier, P. and Kovacic, H., 2021. Tau regulates glioblastoma progression, 3D cell organization, growth and migration via the PI3K-AKT axis. *Cancers*, 13(22), p.5818.

Philips, A., Henshaw, D.L., Lamburn, G. and O'Carroll, M.J., 2018. Brain tumours: rise in glioblastoma multiforme incidence in England 1995–2015 suggests an adverse environmental or lifestyle factor. *Journal of environmental and public health*, 2018.

Powell, S.N. and Kachnic, L.A., 2003. Roles of BRCA1 and BRCA2 in homologous recombination, DNA replication fidelity and the cellular response to ionizing radiation. *Oncogene*, 22(37), pp.5784-5791.

Qiu, C., Kivipelto, M. and Von Strauss, E., 2022. Epidemiology of Alzheimer's disease: occurrence, determinants, and strategies toward intervention. *Dialogues in clinical neuroscience*.

Reardon, S., 2023. Alzheimer's drug donanemab: what promising trial means for treatments. *Nature*, 617(7960), pp.232-233.

Rosenberg, R.N. ed., 2008. *The molecular and genetic basis of neurologic and psychiatric disease*. Lippincott Williams & Wilkins.

Roy, R., Chun, J. and Powell, S.N., 2012. BRCA1 and BRCA2: different roles in a common pathway of genome protection. *Nature Reviews Cancer*, 12(1), pp.68-78.

Sadot, E., Gurwitz, D., Barg, J., Behar, L., Ginzburg, I. and Fisher, A., 1996. Activation of m1 muscarinic acetylcholine receptor regulates τ phosphorylation in transfected PC12 cells. *Journal of neurochemistry*, 66(2), pp.877-880.

Saleh, R.N.M., Hornberger, M., Ritchie, C.W. and Minihane, A.M. (2023). Hormone replacement therapy is associated with improved cognition and larger brain volumes in at-risk APOE4 women: results from the European Prevention of Alzheimer's Disease (EPAD) cohort. *Alzheimer's Research & Therapy*, 15(1). doi:<https://doi.org/10.1186/s13195-022-01121-5>.

Sanganee, A. (2023). *US regulator expands access to Alzheimer's drug lecanemab*. [online] Alzheimer's Research UK. Available at: <https://www.alzheimersresearchuk.org/us-regulator-expands-access-to-alzheimers-drug-lecanemab/> [Accessed 11 Dec. 2023].

Shumaker, S.A., Legault, C., Kuller, L., Rapp, S.R., Thal, L., Lane, D.S., Fillit, H., Stefanick, M.L., Hendrix, S.L., Lewis, C.E. and Masaki, K., 2004. Conjugated equine estrogens and incidence of probable dementia and mild cognitive impairment in postmenopausal women: Women's Health Initiative Memory Study. *Jama*, 291(24), pp.2947-2958.

Stoyanov, G.S., Lyutfi, E., Georgieva, R., Georgiev, R., Dzhenkov, D.L., Petkova, L., Ivanov, B.D., Kaprelyan, A., Ghenev, P. and Ivanov, B., 2022. Reclassification of glioblastoma multiforme according to the 2021 World Health Organization classification of central nervous system tumors: A single institution report and practical significance. *Cureus*, 14(2).

Soreq, H., Lapidot-Lifson, Y. and Zakut, H., 1991. A role for cholinesterases in tumorigenesis?. *Cancer cells (Cold Spring Harbor, NY: 1989)*, 3(12), pp.511-516.

Terry, A.V. and Buccafusco, J.J., 2003. The cholinergic hypothesis of age and Alzheimer's disease-related cognitive deficits: recent challenges and their implications for novel drug development. *Journal of Pharmacology and Experimental Therapeutics*, 306(3), pp.821-827.

Thompson, E.G. and Sontheimer, H., 2019. Acetylcholine receptor activation as a modulator of glioblastoma invasion. *Cells*, 8(10), p.1203.

Tomita, S., Kirino, Y. and Suzuki, T., 1998. A basic amino acid in the cytoplasmic domain of Alzheimer's β -amyloid precursor protein (APP) is essential for cleavage of APP at the α -site. *Journal of Biological Chemistry*, 273(30), pp.19304-19310.

Vassilakopoulou, M., Won, M., Curran, W.J., Souhami, L., Prados, M.D., Langer, C.J., Rimm, D.L., Hanna, J.A., Neumeister, V.M., Melian, E. and Diaz, A.Z., 2021. BRCA1 Protein Expression Predicts Survival in Glioblastoma Patients from an NRG Oncology RTOG Cohort. *Oncology*, 99(9), pp.580-588.

Verger, A., Yakushev, I., Albert, N.L., van Berckel, B., Brendel, M., Cecchin, D., Fernandez, P.A., Fraioli, F., Guedj, E., Morbelli, S. and Tolboom, N., 2023. FDA approval of lecanemab: the real start of widespread amyloid PET use?—the EANM Neuroimaging Committee perspective. *European Journal of Nuclear Medicine and Molecular Imaging*, 50(6), pp.1553-1555.

Walter, F.M., Penfold, C., Joannides, A., Saji, S., Johnson, M., Watts, C., Brodbelt, A., Jenkinson, M.D., Price, S.J., Hamilton, W. and Scott, S.E., 2019. Missed opportunities for diagnosing brain tumours in primary care: a qualitative study of patient experiences. *British Journal of General Practice*, 69(681), pp.e224-e235.

Welsh, J.W., Ellsworth, R.K., Kumar, R., Fjerstad, K., Martinez, J., Nagel, R.B., Eschbacher, J. and Stea, B., 2009. Rad51 protein expression and survival in patients with glioblastoma multiforme. *International Journal of Radiation Oncology* Biology* Physics*, 74(4), pp.1251-1255.

Wen, P.Y. and Packer, R.J., 2021. The 2021 WHO classification of tumors of the central nervous system: clinical implications. *Neuro-oncology*, 23(8), pp.1215-1217.

Wiltfang, J., Smirnov, A., Schnierstein, B., Kelemen, G., Matthies, U., Klafki, H.W., Staufenbiel, M., Hüther, G., Rütger, E. and Kornhuber, J., 1997. Improved electrophoretic separation and immunoblotting of beta-amyloid (A β) peptides 1–40, 1–42, and 1–43. *Electrophoresis*, 18(3-4), pp.527-532.

World Health Organization (2021). *Dementia*. [online] Who.int. Available at:<https://www.who.int/news-room/fact-sheets/detail/dementia>.

Xenabrowser.net. 2022. *UCSC Xena*. [online] Available at: <https://xenabrowser.net/> [Accessed 17 August 2022].

Yiannopoulou, K.G. and Papageorgiou, S.G., 2020. Current and Future Treatments in Alzheimer Disease: An Update. *Journal of Central Nervous System Disease*, 12, p.1179573520907397.

Yilmazer-Hanke, D.M. and Hanke, J., 1999. Progression of Alzheimer-related neuritic plaque pathology in the entorhinal region, perirhinal cortex and hippocampal formation. *Dementia and geriatric cognitive disorders*, 10(2), pp.70-76.

Zayas-Santiago, A., Díaz-García, A., Nuñez-Rodríguez, R. and Inyushin, M., 2020. Accumulation of amyloid beta in human glioblastomas. *Clinical & Experimental Immunology*, 202(3), pp.325-334.

Zhang, X.X., Tian, Y., Wang, Z.T., Ma, Y.H., Tan, L. and Yu, J.T., 2021. The epidemiology of Alzheimer's disease modifiable risk factors and prevention. *The Journal of Prevention of Alzheimer's Disease*, 8(3), pp.313-321.

Zhang, Y., Chen, H., Li, R., Sterling, K. and Song, W., 2023. Amyloid β -based therapy for Alzheimer's disease: Challenges, successes and future. *Signal transduction and targeted therapy*, 8(1), p.248.

Zhao, S., Lin, Y., Xu, W., Jiang, W., Zha, Z., Wang, P., Yu, W., Li, Z., Gong, L., Peng, Y. and Ding, J., 2009. Glioma-derived mutations in IDH1 dominantly inhibit IDH1 catalytic activity and induce HIF-1 α . *Science*, 324(5924), pp.261-265.

Zhou, B., Lu, J.G., Siddu, A., Wernig, M. and Südhof, T.C., 2022. Synaptogenic effect of APP-Swedish mutation in familial Alzheimer's disease. *Science translational medicine*, 14(667), p.eabn9380.

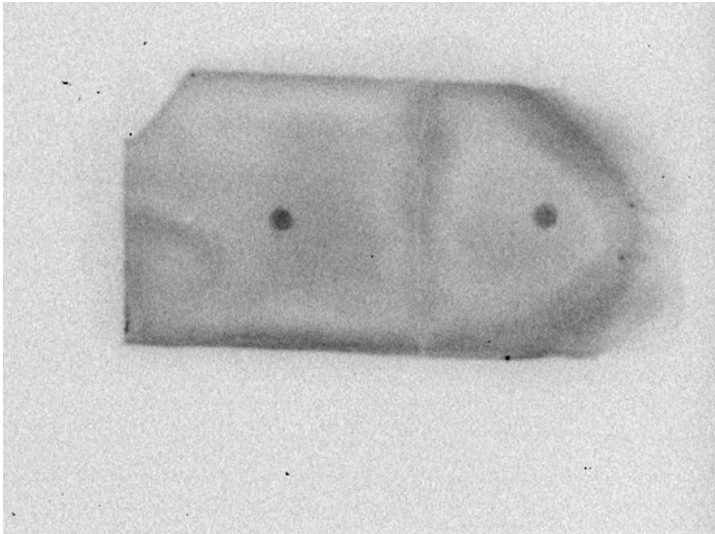
Zhong, Z., Quon, D., Higgins, L.S., Higaki, J. and Cordell, B., 1994. Increased amyloid production from aberrant beta-amyloid precursor proteins. *Journal of Biological Chemistry*, 269(16), pp.12179-12184.

Zigman, W.B., Devenny, D.A., Krinsky-McHale, S.J., Jenkins, E.C., Urv, T.K., Wegiel, J., Schupf, N. and Silverman, W., 2008. Alzheimer's disease in adults with Down syndrome. *International review of research in mental retardation*, 36, pp.103-145.

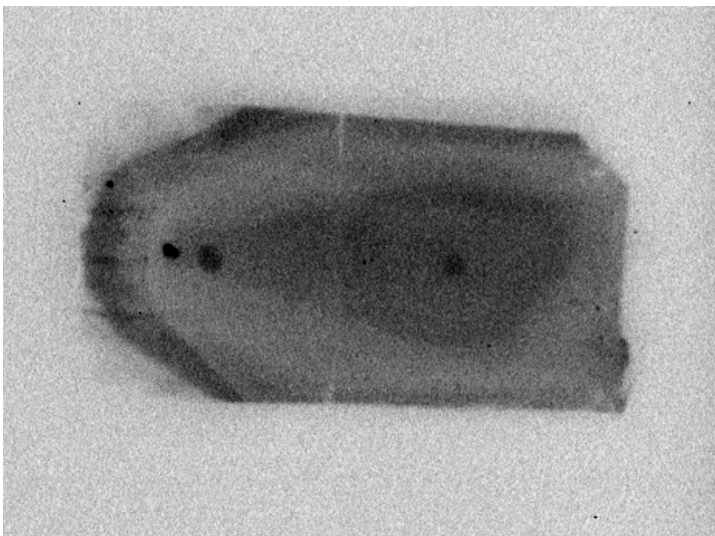
CHAPTER 6

APPENDIX

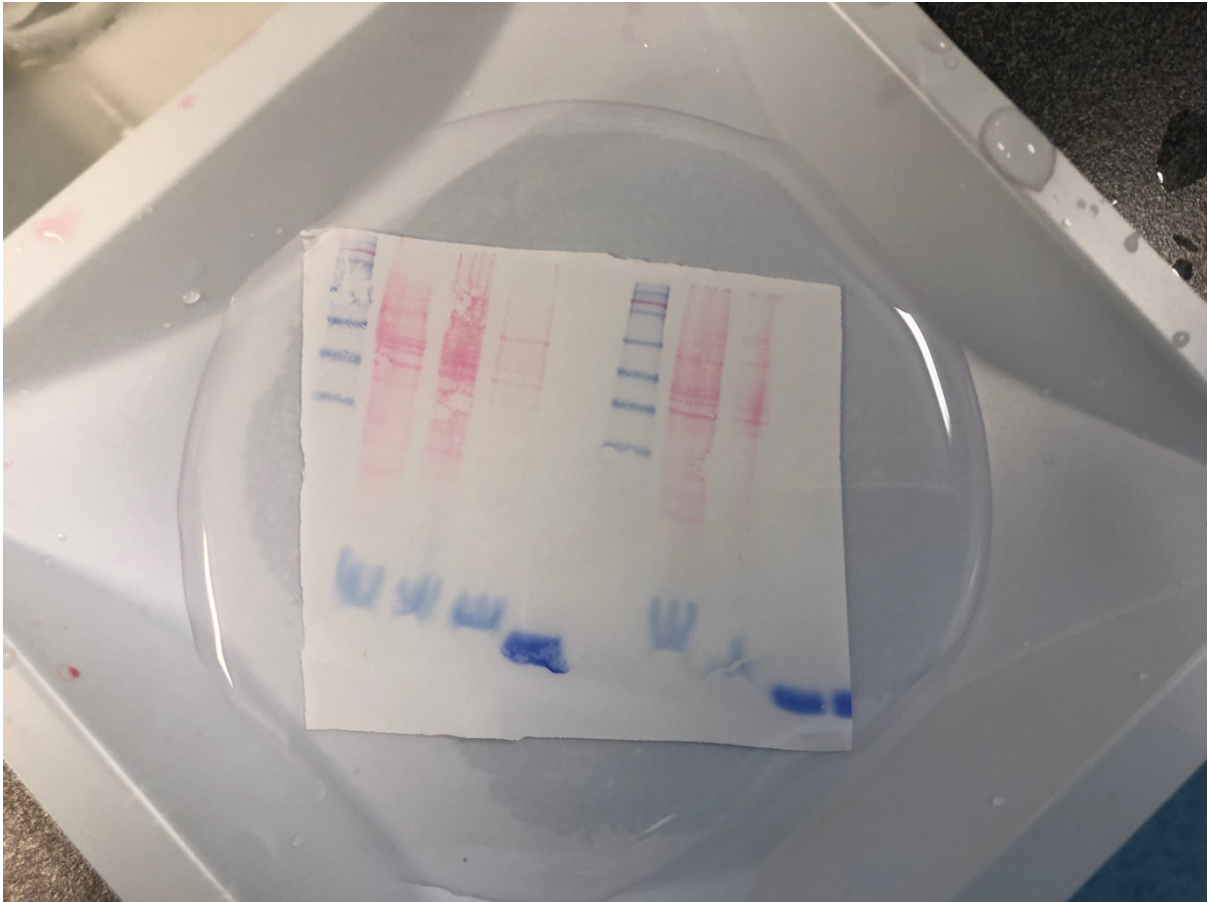
Appendix 1



Appendix 1.1; dot blot of A β 40 stain on 1321N1 (left) and U-87mg (right)



Appendix 1.2; dot blot of A β 42 stain on 1321 (left) and U-87mg (right)



Appendix 1.3; ponceau S stain showing transfer of proteins

Appendix 2.1

Figure 2.1, Graph A, B and C on figure 1.1 revealed no statistical difference between passages ($F_{2,6} = 1.041, p > 0.05$), ($F_{2,6} = 1.3, p > 0.05$) and ($F_{2,6} = 0.02496, p > 0.05$) respectively. In graph D there appears to not have any statistical difference between 1321N1, U-87mg and SVGp12 ($F_{2,6} = 1.263, p > 0.05$).

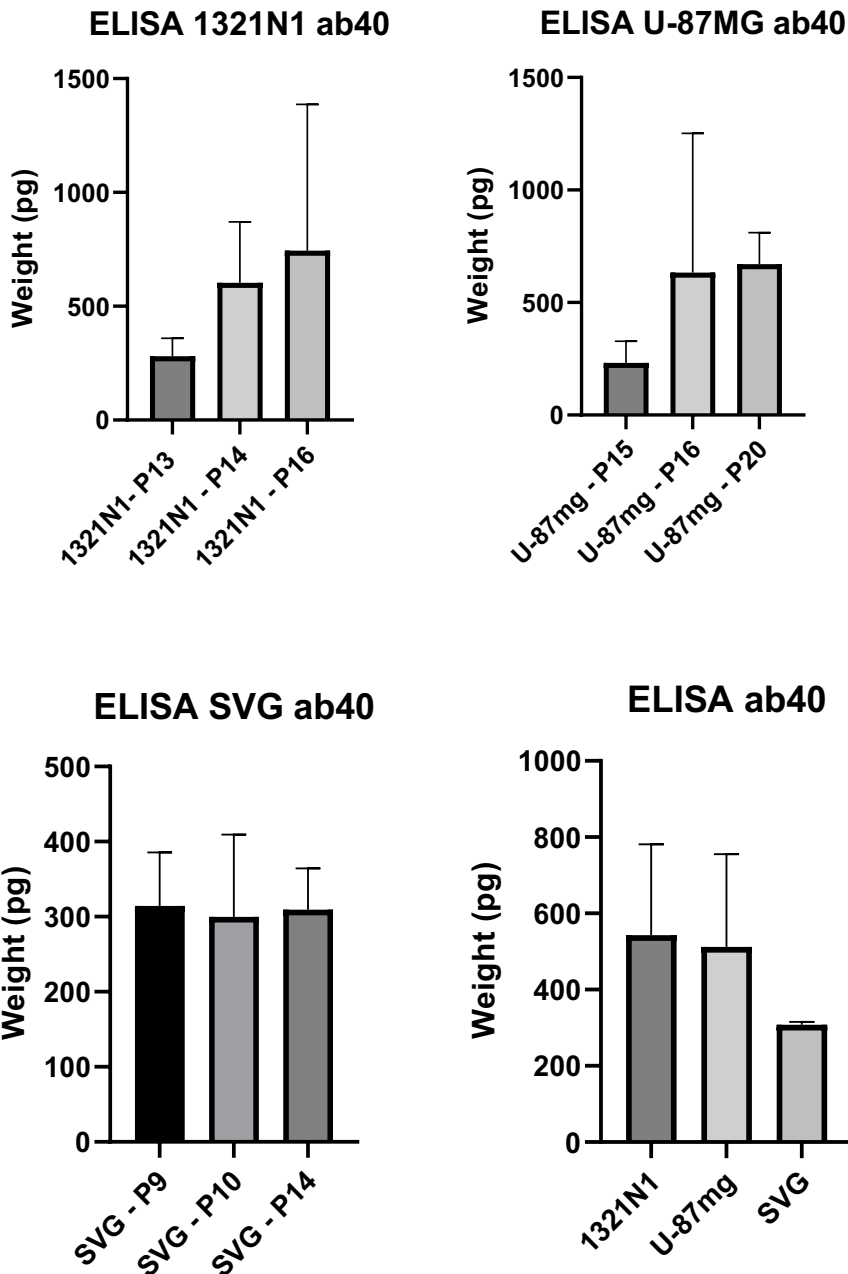


Figure 2.1; Aβ40 Elisa (A) 1321N1, (B) U-87mg (C) SVGp12 and (D) Average of 1321N1, U-87mg and SVGp12

Appendix 2.2

Figure 2.2, The statistical results on figure 1.2 indicates that graph A, B, C and D have ns. A ($F_{2,6} = 3.513, p > 0.05$), B ($F_{2,6} = 3.548, p > 0.05$), C ($F_{2,6} = 3.342, p > 0.05$) and D ($F_{2,6} = 0.8864, p > 0.05$).

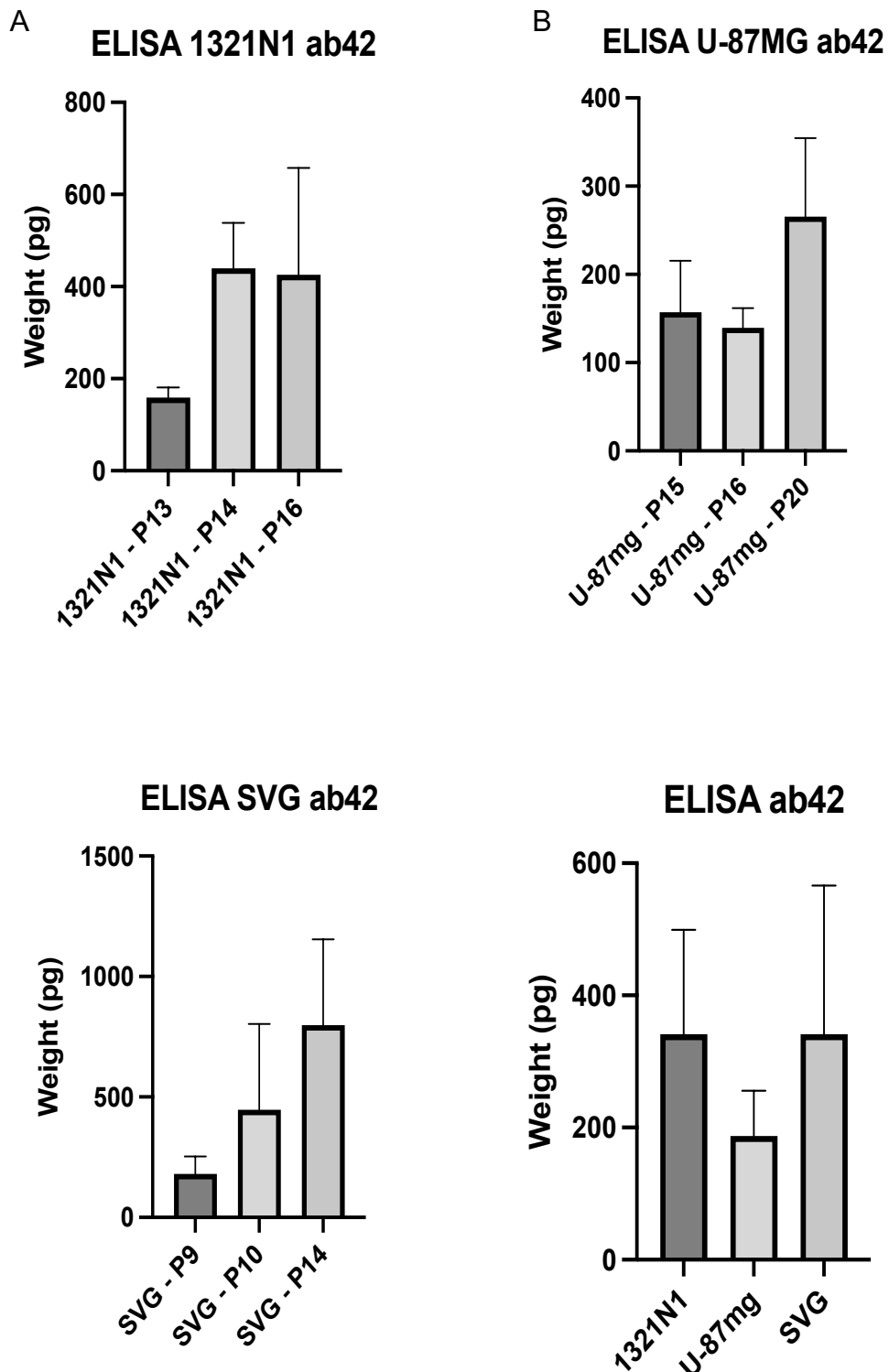


Figure 2.2; Aβ42 Elisa (A) 1321N1, (B) U-87mg (C) SVGp12 and (D) Average of 1321N1, U-87mg and SVGp12

Effect of amyloid inhibition on glioma cell growth

Appendix 2.

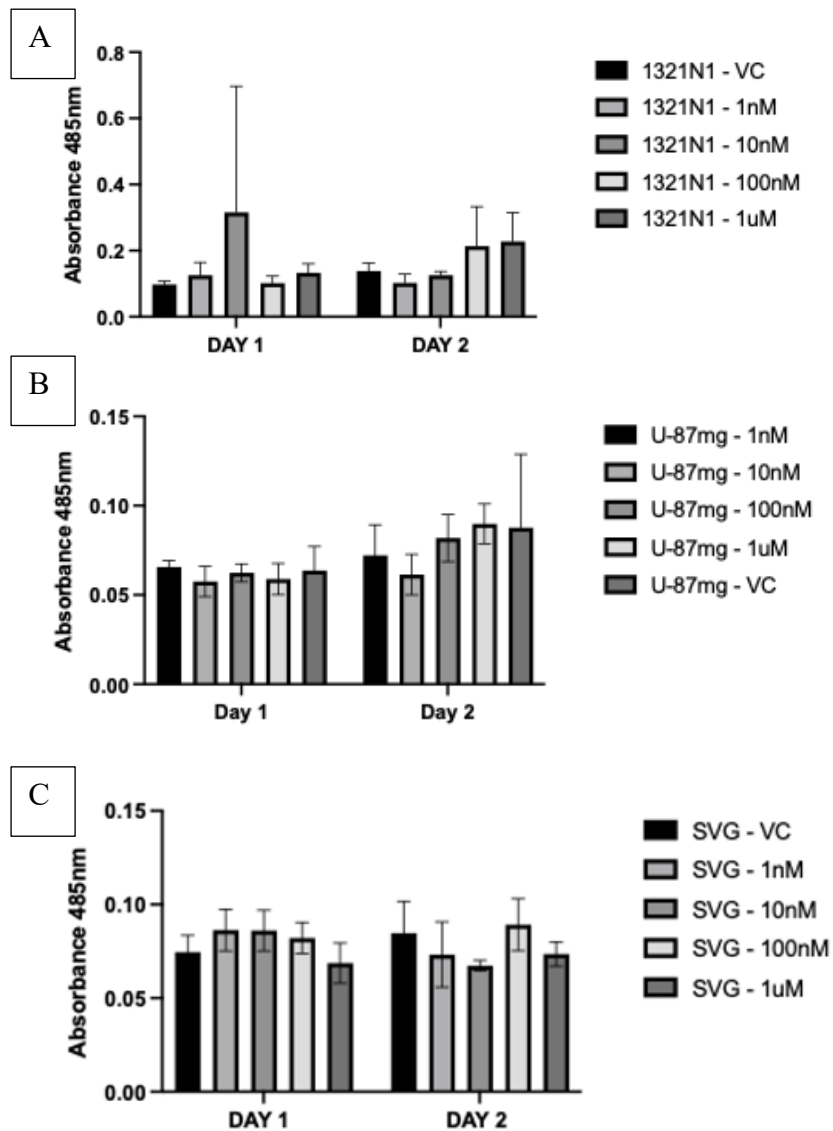


Figure 2.3; The results of the inhibitor concentration optimisation showed no statistical difference in comparison to the control. (A) 1321N1 ($F_{4,20} = 1.302$, $p > 0.05$), (B)U-87MG ($F_{4,20} = 0.7115$, $p > 0.05$) and (C) SVGp12 ($F_{4,20} = 1.891$, $p > 0.05$).

Appendix 2.

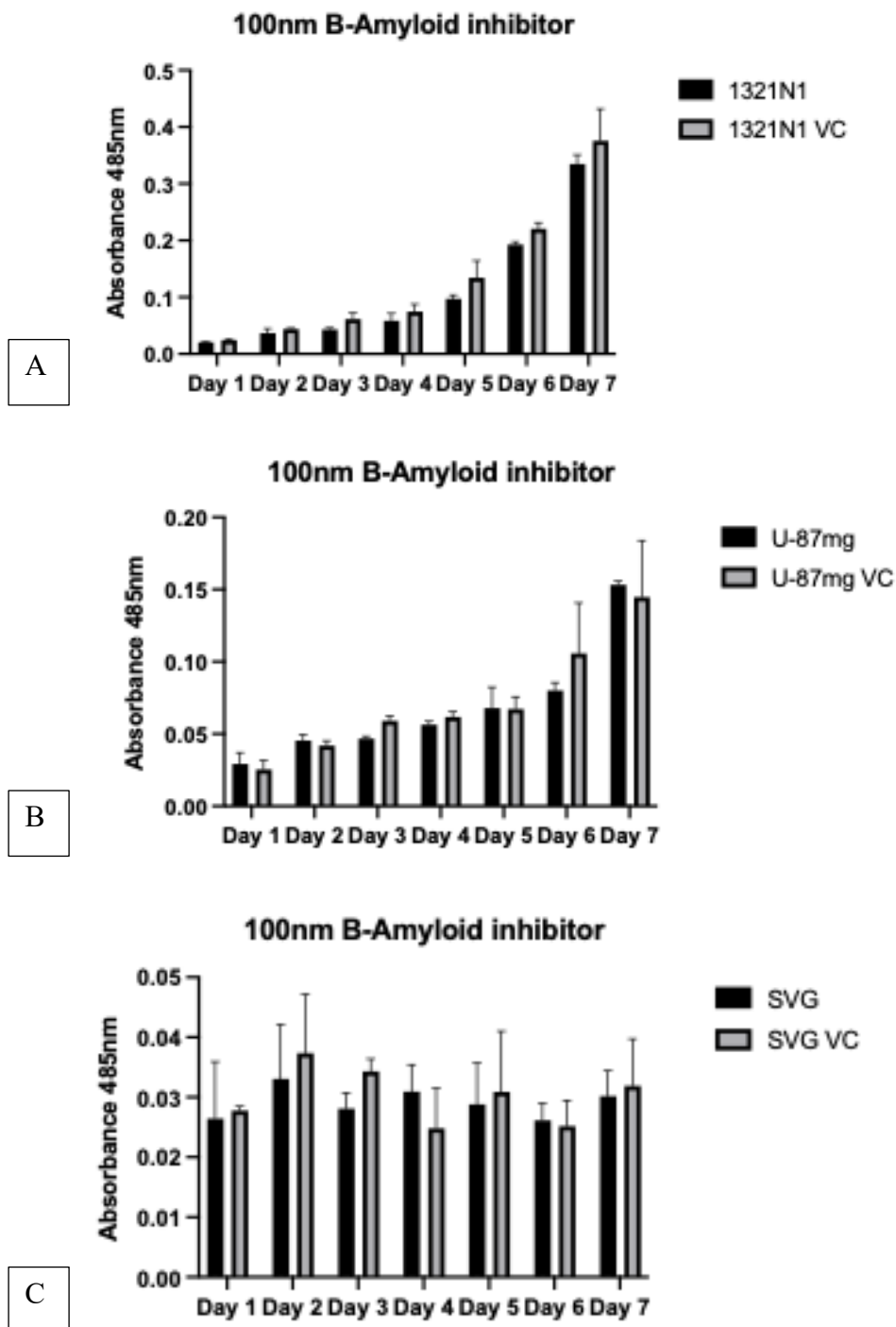


Figure 2.4, Graph A, B and C showed no significance. (A) 1321N1 ($F_{6,28} = 0.8539$, $p > 0.05$), (B) U-87MG ($F_{6,28} = 0.8996$, $p > 0.05$) and (C) SVGp12 ($F_{6,28} = 0.5472$, $p > 0.05$).

Appendix 3.

Bioinformatic exploration of amyloid associated proteins

As explained in method, the outliers were investigated further from Table 1

% Rank			
GENES	LGG	GENES	GBM
<i>TARDBP</i>	421.329633	<i>TARDBP</i>	418.219668
<i>CDKN2A</i>	134.842746	<i>EXOC3L2</i>	189.461445
<i>TREM2</i>	134.199879	<i>SERPINA3</i>	163.463825
<i>BCHE</i>	132.337625	<i>PLAU</i>	159.998097
<i>SERPINA3</i>	126.538729	<i>IL1A</i>	156.120202
<i>TP53</i>	123.022	<i>TREM2</i>	150.572863
<i>IL1B</i>	120.43452	<i>MS4A6A</i>	147.121993
<i>BRCA2</i>	118.193577	<i>IL1B</i>	145.809564
<i>MS4A6A</i>	117.06	<i>BRCA2</i>	145.522977
<i>HLA-DRB1</i>	111.388778	<i>CDKN2A</i>	130.155976
<i>PMS2</i>	111.332792	<i>TP53</i>	130.060382
<i>PLAU</i>	111.081097	<i>HLA-DRB1</i>	129.33503
<i>CDK4</i>	109.671437	<i>DSG2</i>	128.757164
<i>EGFR</i>	109.378876	<i>BCHE</i>	126.372347
<i>IDH1</i>	109.029232	<i>CD33</i>	125.649419
<i>CD33</i>	108.497793	<i>CDK4</i>	120.900251
<i>A2M</i>	107.426621	<i>IDH1</i>	116.99195
<i>IL1A</i>	106.943355	<i>EGFR</i>	115.623278
<i>RIN3</i>	106.609799	<i>IL6</i>	114.782271
<i>APOE</i>	105.319	<i>A2M</i>	113.174399
<i>HSD17B10</i>	105.068137	<i>BACE2</i>	110.90249
<i>GFAP</i>	104.090549	<i>HSD17B10</i>	110.566446
<i>LRP1</i>	102.152	<i>RIN3</i>	110.560792
<i>NRAS</i>	101.857204	<i>NRAS</i>	109.807892
<i>INPP5D</i>	101.316799	<i>PMS2</i>	109.749198
<i>CLU</i>	101.313	<i>CASP3</i>	108.414124
<i>SORL1</i>	101.261182	<i>HFE</i>	108.164703
<i>COMT</i>	101.042424	<i>PTGS2</i>	105.341728
<i>DBN1</i>	100.293249	<i>MDM2</i>	103.636679
<i>CTSD</i>	99.4223751	<i>INPP5D</i>	103.624676
<i>FERMT2</i>	99.1311634	<i>CLU</i>	103.448711
<i>PSENEN</i>	98.9419385	<i>CTSD</i>	103.429681
<i>PSEN1</i>	98.452	<i>ERBB2</i>	103.397544
<i>APP</i>	98.203	<i>PSENEN</i>	103.181995
<i>IDH2</i>	97.9404079	<i>FERMT2</i>	102.47655
<i>ERBB2</i>	97.8081893	<i>GFAP</i>	101.943869
<i>BACE1</i>	97.0511885	<i>CR1</i>	100.66612
<i>MAPT</i>	97.042583	<i>APOE</i>	100.399159
<i>CASP3</i>	96.7316789	<i>MAOB</i>	100.305102
<i>MDM2</i>	96.4944272	<i>COMT</i>	99.8481818

<i>APLP2</i>	96.4304736	<i>LRP1</i>	98.8259701
<i>GSK3B</i>	96.3999757	<i>IDH2</i>	98.3337688
<i>MEF2C</i>	96.2493312	<i>UBB</i>	98.247756
<i>PICALM</i>	95.244	<i>DBN1</i>	98.195101
<i>KRAS</i>	95.1043161	<i>PSEN1</i>	97.9350124
<i>MSH2</i>	93.8558462	<i>APP</i>	97.6299249
<i>MTOR</i>	93.6586802	<i>MSH2</i>	97.5741953
<i>TF</i>	92.861	<i>APLP2</i>	97.4750576
<i>RPS27A</i>	92.371512	<i>PSEN2</i>	97.0418236
<i>TOMM40</i>	92.1903327	<i>PICALM</i>	96.0110246
<i>PRNP</i>	92.0592371	<i>MEF2C</i>	95.7497822
<i>UBB</i>	91.8720397	<i>CASS4</i>	95.1523499
<i>SOD1</i>	91.4754459	<i>BACE1</i>	94.5787625
<i>PSEN2</i>	90.90406	<i>TOMM40</i>	94.1101691
<i>ZCWPW1</i>	90.7463234	<i>APBA3</i>	93.4866342
<i>CDK5R1</i>	90.5546331	<i>FGFR1</i>	93.084689
<i>CASS4</i>	89.5994301	<i>PLD3</i>	92.9438146
<i>CELF1</i>	89.5354974	<i>SORL1</i>	92.7085688
<i>GSK3A</i>	89.4503677	<i>KRAS</i>	92.5893778
<i>PLD3</i>	89.2243284	<i>GSK3B</i>	92.5187563
<i>ADAM10</i>	89.0356211	<i>MTOR</i>	91.668986
<i>BACE2</i>	88.785	<i>SOD1</i>	91.3774065
<i>FGFR1</i>	88.5676537	<i>GSK3A</i>	91.1043619
<i>CD2AP</i>	88.4069513	<i>CD2AP</i>	90.6337526
<i>PTEN</i>	88.3090356	<i>ATRX</i>	90.2797525
<i>LRRK2</i>	88.1000985	<i>ADAM10</i>	90.1347347
<i>APBA3</i>	88.0465921	<i>LRRK2</i>	90.0405393
<i>BIN1</i>	87.5625918	<i>PRNP</i>	89.667256
<i>PIK3CA</i>	86.6814967	<i>PPARG</i>	88.4220091
<i>HRAS</i>	85.8355146	<i>UCHL1</i>	88.0901539
<i>SYP</i>	85.1879123	<i>CELF1</i>	86.3438697
<i>APBB3</i>	84.2818798	<i>HRAS</i>	86.1512664
<i>UCHL1</i>	84.1429696	<i>RPS27A</i>	84.5465461
<i>MAOB</i>	84.1375385	<i>PTEN</i>	84.5212551
<i>IDE</i>	83.8542788	<i>MAPT</i>	84.3583546
<i>SLC24A4</i>	82.8032546	<i>IDE</i>	83.2373736
<i>AGER</i>	81.2527097	<i>MGMT</i>	83.0260573
<i>PTK2B</i>	79.8213491	<i>PIK3CA</i>	83.0077777
<i>PTGS2</i>	79.608015	<i>APBB3</i>	82.699414
<i>HTR2A</i>	79.016	<i>NOS3</i>	82.4185634
<i>NOS3</i>	78.9066262	<i>BIN1</i>	81.9580336
<i>ACHE</i>	78.3978886	<i>ZCWPW1</i>	81.7823849
<i>HFE</i>	75.919465	<i>TF</i>	81.651692
<i>EXOC3L2</i>	75.553	<i>PTK2B</i>	80.2166979
<i>PPARG</i>	74.3525837	<i>AGER</i>	80.1364733
<i>MGMT</i>	73.3223901	<i>CDK5R1</i>	78.3763315
<i>SNCB</i>	73.2283484	<i>ACHE</i>	77.2499475
<i>SNCA</i>	73.1096996	<i>BDNF</i>	76.2292468

<i>ABCA7</i>	71.9731444	<i>COL25A1</i>	75.1192555
<i>CR1</i>	69.5101039	<i>SYP</i>	74.6948202
<i>BDNF</i>	68.7904476	<i>ABCA7</i>	70.7361368
<i>MME</i>	67.3649311	<i>SNCA</i>	68.5316314
<i>COL25A1</i>	64.8558527	<i>MME</i>	67.2737035
<i>NGF</i>	62.9120774	<i>NGF</i>	65.4245926
<i>IL6</i>	62.1071835	<i>SLC24A4</i>	64.1798387
<i>BRAF</i>	61.9438434	<i>BRAF</i>	62.0643798
<i>CHRNA7</i>	59.519155	<i>SNCB</i>	60.6936294
<i>DSG2</i>	58.9466699	<i>HTR2A</i>	54.6687959
<i>CYP2D6</i>	51.4935981	<i>CHRNA7</i>	53.1825077
<i>UNC5C</i>	50.5350534	<i>MPO</i>	48.850305
<i>CALHM1</i>	47.2185391	<i>UNC5C</i>	45.9745641
<i>MPO</i>	43.7189027	<i>CHAT</i>	43.1252557
<i>EPHA1</i>	26.0285563	<i>EPHA1</i>	42.3328142
<i>DRD3</i>	25.9918545	<i>CALHM1</i>	33.066379
<i>CHAT</i>	25.5410448	<i>CYP2D6</i>	28.212604
<i>ATRX</i>	2.61	<i>DRD3</i>	22.0334844

Table 2: Expression of closeness 106 genes in LGG and GBM to normal samples

Appendix 3.

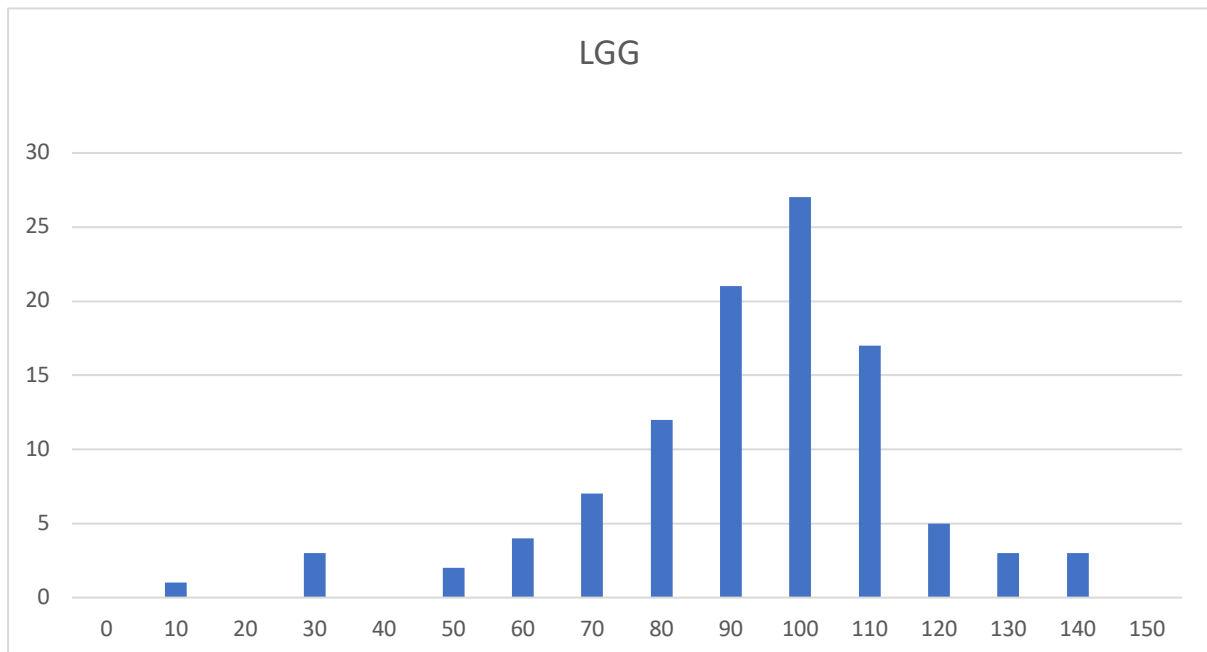


Figure 3.1; Gene expression in LGG samples in closeness to normal samples.

Appendix 3.

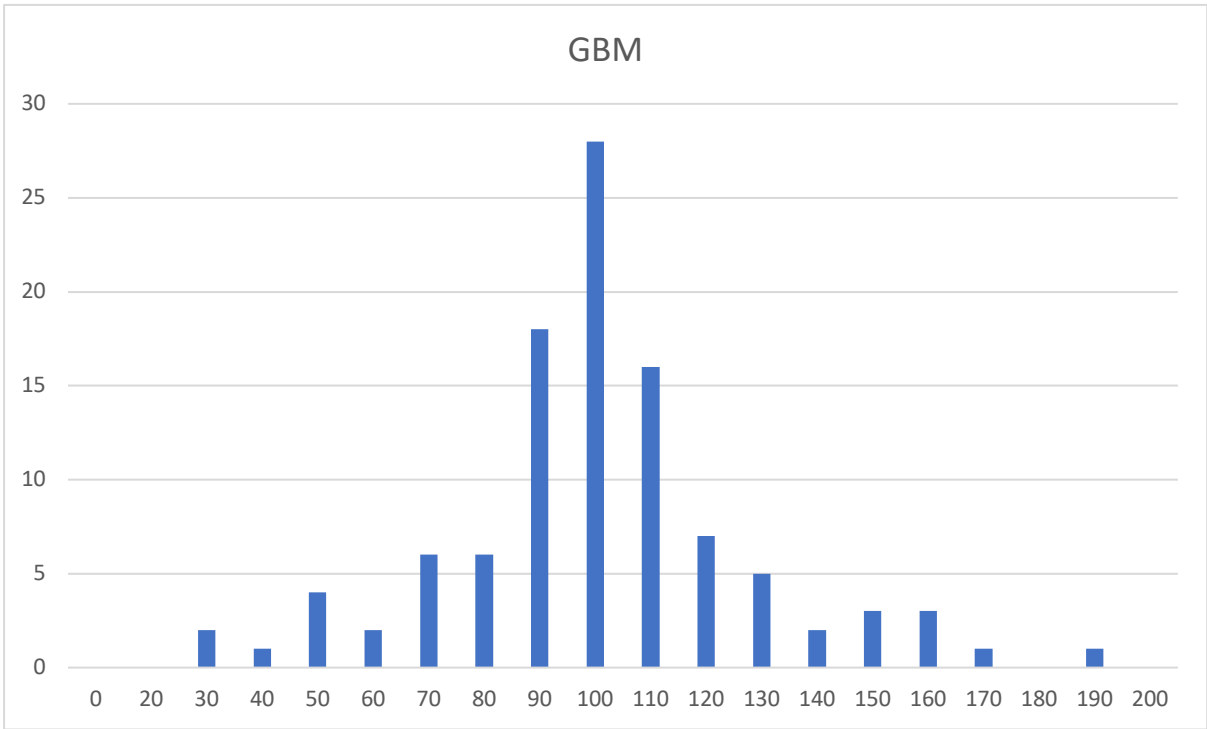


Figure 3.2; Gene expression in GBM samples in closeness to normal samples.

Appendix 3.

Genes	P value (Kaplan Meier)	F value (Box plot)
ATRX	0.01306	11.9
COL25A1	0.2761	29.44
DRD3	0.1317	38.93
MME	0.0001093	42.36
CHRNA7	0.000000075660000000	45.51
NGF	0.6951	48.76
CR1	0.00000683	49.39
HTR2A	6.88E-15	56.09
BDNF	0.002595	73.29
IL6	1.44E-15	79.62
BRAF	7.64E-07	97.66
IL1A	1.38E-09	190.7
IL1B	6.60E-07	246.5
CALHM1	0.000010300000000000	262.60
CD33	7.93E-07	285.7
EXOC3L2	0.00000000000000011100	349.20
SERPINA3	2.44E-11	354.70
UNC5C	0.9726	355.7
HLA-DRB1	3.54E-09	447.7
MS4A6A	0.000000136500000000	525.40
SNCB	0.0004761	526
CYP246	0.000009191000000000	612.80
CYP2D6	0.000009191	612.8
PLAU	0.000000000312300000	751.00
SNCA	0.02413	775.1
MPO	0.1201	893.1
TREM2	0.101053000000000000	903.00
BRCA2	0.0000289	1210
CDK4	0.08923	1268
TP53	0.06856	1807
BCHE	0.005855000000000000	2033.00

Figure 3.3; 30 genes chosen with P value of Kaplan Meier and F value One-way anova

Appendix 4.

Buffers

RIPA Buffer (250ml) – Lysis buffer

<u>250ml</u>	<u>50ml</u>
50mM Tris – pH = 1.7g 150mM NaCL = 2.1g 0.5% Sodium deoxycholate = 1.25g 1% Triton = 2.5ml	50mM Tris – pH = 0.394 150mM NaCL = 0.438g 0.5% Sodium deoxycholate = 0.25g 1% Triton = 0.5ml

Store at 4°C

(+ 1x protease inhibitor **prior to use**) – 100ul (1 vial) per 10ml RIPA

2.5M Tris-HCL buffer (pH 8.8)

Tris base – 302.85g
Deionized water – 600 mL
HCL – adjust pH to 8.8

Make up to 1 L. Store at 4-8 °C.

Ammonium persulphate (APS)

APS – 0.1g
H₂O – 1ml

Make up fresh.

Urea (6M) = 3.6036g

Sample or loading buffer

1% (w/v) SDS = 100 ul (0.1g)
24% glycerol (v/v) = 2.4 ml
0.02% (w/v) Coomassie Brilliant Blue = 2 ul (0.002g)
100mM Tris-HCL (pH 6.8) = 0.1576g – (0.12114g Tris & 0.03646g HCL)

Make up to 10ml with dH₂O. Adjust ph to 6.8(buffer should be dark blue)

Aliquot and store at -20°C

Add 4% mercaptoethanol prior to use – use fume hood!

Running buffer x10 (1 litre)

25mM Tris = **3.03g**
25 mM Tricine = **4.5g**
0.05% (W/V) SDS = **0.5g**

Make up to 1L with distilled water

There is no need to adjust the pH. **Store at 4–8°C**

STORE AT RT

Transfer buffer x10 (1 litre) pH 8.3 > (do not add acid or base to correct running buffer)

25mM Tris = **30.4g**
190mM glycine = **144.2g**
Make up to 1L with distilled water.

STORE AT RT

For working concentrations

Dilute to x1 (80mL x10 Transfer buffer + 720ml dH₂O)
Then add 200ml Methanol to make up 1L

TBS x10 (1L) pH7.6

20mM Tris – pH7.5 = **24.2g**
150mM NaCl = **87.6g**
Make up to 1L with distilled water. Adjust pH to 7.6

TBST x1 (1L)

100ml TBS x10
900ml distilled water
1ml Tween
STORE AT 4°C

Blocking solution (20ml)

5% milk powder = **1g**
20ml TBST

STORE AT 4°C – (Can be made as blot is running)

Stripping buffer

15g glycine
1g SDS or 10ml of 10% to make 0.1% solution
10ml Tween
Adjust pH to 2.2
 Add H₂O up to 1L

		4% sample gel	10% gel	16% gel	16%/6 M urea
AB-3	(ml)	1	6	10	10
Gel buffer (3×)	(ml)	3	10	10	10
Glycerol	(g)	—	3	3	—
Urea	(g)	—	—	—	10.8
Add water to final volume	(ml)	12	30	30	30
Polymerize by adding:					
APS (10%)	(μl)	90	150	100	100
TEMED	(μl)	9	15	10	10

Table 4.1; hand cast gel composition (Schägger, 2006)

Percentage of acrylamide in the gel		Acrylamide/ bis-acrylamide 29:1 30% (w/v) solution (mL)	2.5 M Tris buffer (pH 8.8 for modified and pH 8.45 for original method) (mL)	Deionized water (mL)	TEMED (μL)	APS 30 mg/mL μL	Total volume (mL)
Stacking gel	4	0.66	0.76	3.42	5.0	150	~5
Resolving gel	7	2.33	5.6	1.91	7.0	150	~10
	9	3.00	5.6	1.24	6.0	150	~10
	10	3.33	5.6	0.90	6.0	150	~10
	12	4.00	5.0	0.89	6.0	100	~10
	15	5.00	4.6	0.29	6.0	100	~10
	16	5.33	4.3	0.22	6.0	100	~10

Table 4.2; hand cast gel composition (Haider et al.,2012)